The Application of Liposomes in Synthetic Biology

Jacqueline Brauneis

Masters Report

Biomedical Engineering

STATEMENT BY AUTHOR

This thesis has been submitted in partial fulfillment of requirements for an advanced degree at The University of Arizona and is deposited in the University Library to be made available to borrowers under rules of the Library.

Brief quotations from this thesis are allowable without special permission, provided that accurate acknowledgment of source is made. Requests for permission for extended quotation from or reproduction of this manuscript in whole or in part may be granted by the head of the major department or the Dean of the Graduate College when in his or her judgment the proposed use of the material is in the interests of scholarship. In all other instances, however, permission must be obtained from the author.

SIGNED: 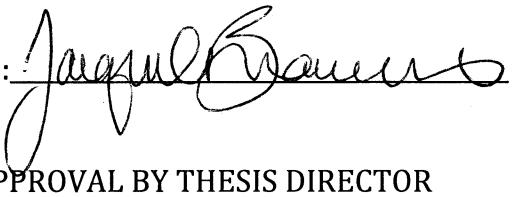

APPROVAL BY THESIS DIRECTOR

This thesis has been approved on the date shown below:

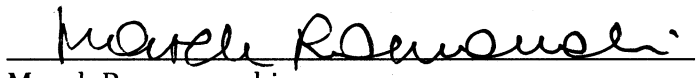

Marek Romanowski

5/2/2012

Date

Table of Contents

List of Tables

List of Figures

List of Abbreviations

ATP	Adenosine triphosphate
CCD	Charged couple device
CPR	Cytochrome P450 reductase
CW	Continuous wave
CYP71AV1	4,11-diene monooxygenase
DDAO	Lauryldimethylamine oxide
DLPC	Dilauroyl phosphatidylcholine

DPA	Diphenylamine
DPPC	Dipalmitoyl phosphatidylcholine
DPPE	Dipalmitoyl Phosphatidylethanolamine
EMCCD	Electron multiplying charge coupled device
FDP	Farnesyl diphosphate
FfAME	Foundation for Applied Molecular Evolution
FPP	Flexible polypropylene
GFP	Green fluorescent protein
GUV	Giant unilamellar vesicle
iGEM	International Genetically Engineered Machine
IR	Infrared
LED	Light emitting diode
LUV	Large unilamellar vesicle
MPPC	Monopalmitoyl phosphatidylcholine
NA	Numerical aperture
NIH	National Institutes of Health
NIR	Near infrared
PEEK	Polyetheretherketone
PEG	Polyethylene glycol
PMMA	Polymethylmethacrylate
PSSH	Psuedo-steady-state hypothesis
SLM	Spatial light modulator
T7 RNAP	Ribonucleic acid polymerase from the T7 bacteriophage

TCPO	bis(2,4,6-trichlorophenyl)oxalate
TWIST	The Westheimer Institute of Science and Technology

Abstract

In the emerging field of synthetic biology, researchers are synthesizing artificial cells that are able to perform novel functions and produce useful products. However, the current methods for the synthesis of these cells are time-consuming and restrictive. This report proposes a novel approach to artificial cell synthesis by means of an assembly line embedded within a microfluidic chip in which components are loaded into an empty synthetic cell membrane. The components are able to be loaded via an optical trapping system capable of maneuvering liposomes coated in gold nanoparticles. This system will result in an increased production efficiency that can be completely controlled at a reasonable cost.

1. Introduction

Today's scientists are vigorously working to address enormous issues such as world hunger, limited natural resources, and deadly diseases. Although many techniques have been utilized to try and rid the world of these problems, many researchers are turning towards an emerging biological field for guidance: synthetic biology. Whether or not all of these scientists classify their work as being within the synthetic biology realm, they are still related in their attempt to alter cellular function, or to modify naturally occurring biological components into synthetic components that are designed to accomplish a certain task. The most common example of this is genome synthesis, in an attempt to create a synthetic or semi-synthetic cell (depending on whether or not the other components are synthetic as well). This is an appealing goal, because the possibilities are endless. One could create a cell that can produce vaccines, or fuel sources without requiring an energy input other than glucose or sunlight.

Even though this idea of a synthetic genome is pursued by many (and has even been accomplished, as discussed later), the techniques currently employed to insert these genomes into living cells leave much to be desired. Common methods of transfection such as lipofection, in which DNA-containing liposomes fuse with the cell membrane and release their content inside, rely on the spontaneous fusion of the liposome and the cell, and can therefore be time-consuming or undependable. Methods such as electroporation and

photoporation, which make the host cell membrane more porous, rely on the diffusion of content into the porous membrane without any control. Natural methods, such as the utilization of cellular endocytosis mechanisms, depend on natural cellular receptors or the spontaneous encapsulation by the cell membrane, which again is unreliable, and furthermore is impossible if the host cell membrane is synthetic and does not possess natural receptors. Finally, viruses can be used to introduce genome fragments into the host genome through the use of reverse transcription, although it cannot do so unless the host cell provides the correct enzymes, and is again an uncontrollable process. All of these currently used methods have one thing in common: they can not be controlled by an operator. Synthetic genomes, along with other components that comprise a synthetic cell, must be inserted via unreliable processes. If a cell could be built in real-time and in a controlled manner, in a system resembling a cellular-scale "factory", then the synthetic biology world would be changed.

This report proposes a system that utilizes both synthetic biology principles and techniques currently used in the lab, such as optical trapping, to streamline the synthetic cell building process by addressing four specific aims. This first aim of this report is to provide a critical overview of the growing field of synthetic biology (and the concept of a minimal cell) by analyzing the work of some well-known synthetic biologists whose work supports the realization of the desired functions of the proposed system. The second aim is to analyze pertinent uses of liposomes in scientific research, as this is an important

component of the proposed system. The third aim is to describe the optically active liposome and optical trapping technology currently utilized by the Romanowski lab, which will become integrated into the new system. The final aim is to introduce a specific proposal for the development of an assembly line for biologically inspired constructs, and define the goals that it will hypothetically be able to accomplish.

2. Synthetic Biology

As one of the oldest subjects studied by scientists, biology has become more and more mastered over time. However, its complexity and unwieldiness has resulted in a void that has been filled for most other subjects. It is from this void that the field of synthetic biology has developed. Chemists are able to synthesize chemicals due to their understanding of chemicals and their interactions. Physicists can design systems known to adhere to the finite laws of physics. For the past few decades, biologists have similarly attempted to tinker with their field—with the biological laws dictated by nature. Synthetic biologists are attempting to create a new subject, one where life can be created or altered to fit the needs of our society. With enough development in the field, it could someday be possible to manipulate chemicals, produce energy, provide food, or enhance human health with the use of synthesized cells.

There are two main directions that synthetic biologists have taken the field. With the eventual goal of producing a living cell out of completely synthetic parts, the first direction currently serves as a teaching mechanism, allowing synthetic biologists to learn about biological complexities as they attempt to assemble synthetic components in a natural, Darwinian manner. The second aims to create unnatural cells from naturally occurring, or slightly genetically altered interchangeable parts. These synthetic cells are designed to serve a specific purpose, such as to generate vaccines without the requirement of fossil fuels or other costly energy sources.

Bottom-up Synthetic Biology

The first direction is also known as bottom-up synthetic biology, in order to symbolize the building of a cellular system from the ground up. Synthetic biologists working in this field center their studies mainly on the development of minimal cells, or, synthetic cells with the absolute minimum necessary parts and functions to be considered "alive." However, since the definition of "alive" varies greatly across the board, the construction of minimal cells also varies with each researcher. This will be discussed more in the next subsection. Among modeling methods developed by bottom-up synthetic biologists, two are the most relevant to the proposed system—the research done by Petra Schwille, and by Pier Luigi Luisi.

Petra Schwille is a synthetic biologist working at the biotechnology center (Biotec) at TU Dresden in Germany. Schwille is mainly known for her work in the imaging field, especially for her work with fluorescence correlation spectroscopy (Korlach 1999, Schwille 1997, Schwille 1999). However, she also devotes much of her research to the study of lipid membranes, particularly their interaction with proteins. This work demonstrates how GUVs can be used to model functional cellular membranes—a concept that helps to affirm the purpose of the proposed system. One of her most notable articles is one in which her lab used three-dimensional confocal imaging and fluorescence correlation spectroscopy to characterize lipid bilayers of giant unilamellar vesicles (GUV) resulting in the "exact superposition of like phase domains in apposing monolayers" as seen in figure 1 (Korlach 1999).

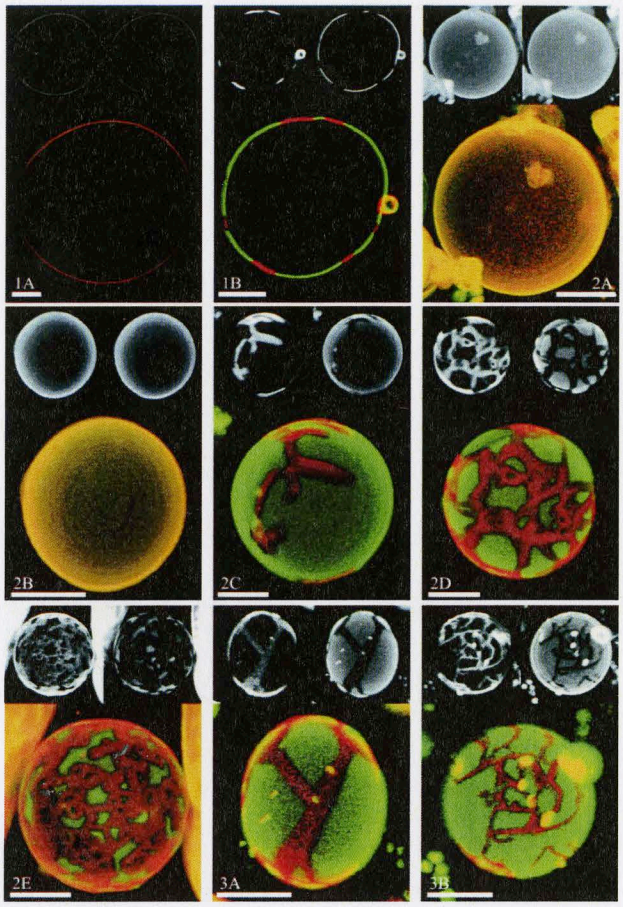

Figure 1. Confocal images of GUVs. 1A shows a single fluid phase DLPC GUV; 1B shows an ordered-fluid two-phase coexistence (0.6 DLPC and 0.4 DPPC); 2A-2E show phase separation in GUVs with varying lipid concentrations (progressing in DPPC/DLPC concentration ratios), note that 2D shows two concentric GUVs to demonstrate the superposition of phase domains in apposing monolayers); 3A and 3B show a 0.5 DPPC and 0.5 DLPC mixture with 0% cholesterol (3A) and 5 mol % cholesterol (3B) (Image from Korlach 1999).

These results are of significance because natural cellular events such as protein sorting, protein aggregation, signaling, and membrane fusion are related to the membrane phase behavior, which is difficult to determine. Characterizing membranes, especially those made

purely from lipids such as those used typically used in the lab, is a way to assure that synthetic membranes closely resemble natural cells. With respect to synthetic biology, one of her lab's most significant contributions is the creation of porcine brain GUVs with an anchored actin filament system meant to mimic a cell's cytoskeleton (Merkle 2008). These cytoskeletons were able to maintain their structure due to the NaOH extraction of the membranes, and were anchored to the interior of the GUVs through the spectrin/ankyrin proteins, which bind to the integral membrane proteins of the GUVs. An elementary image of a cytoskeleton within a GUV is shown below in figure 2.

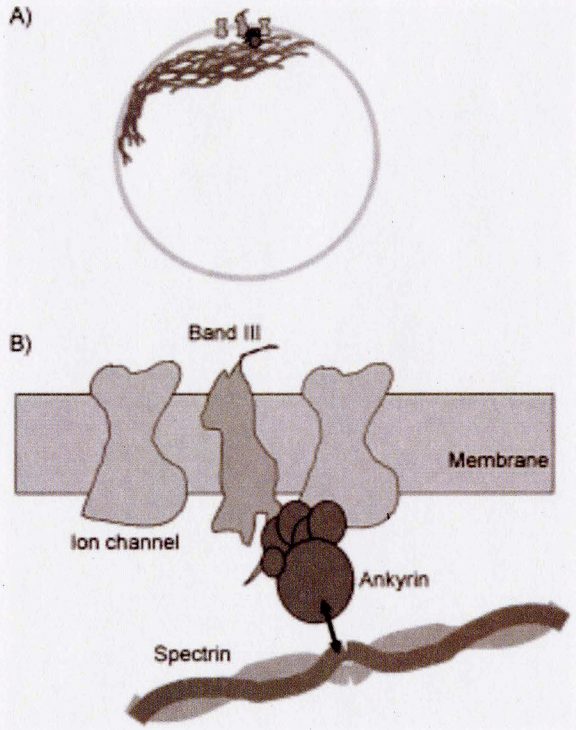

Figure 2. Image A contains a GUV with membrane proteins creating a cytoskeleton. Image B shows a close up of the top of the GUV showing ion channels, Band III, ankyrin, and spectrin, which help to anchor the filaments to the membrane. (Image from Merkle 2008).

As the results of this research served as "the first reconstruction of the natively anchored cytoskeleton to the interior walls of GUVs", this is a significant step in the quest to create a minimal cell, or the simplest version of a self-replicating, fully functional artificial cell. It is necessary for the cytoskeleton to remain organized and anchored throughout cytokinesis, and so the next step in this research is to control the organization of these actin networks in the GUVs and introduce motor proteins to induce constriction of the vesicles (Merkle 2008).

Pier Luigi Luisi is the director of the Synthetic Biology and Supramolecular Chemistry Laboratory at Roma Tre University in Italy, and considers himself to be a natural scientist. He is the author of three texts books, entitled "The Minimal Cell", "Chemical Synthetic Biology", and "The Emergence of Life" (Luisi and Stano 2011, Luisi and Chiarabelli 2011, Luisi 2006). Luisi spends most of his time looking for the "purpose of life within the structure and function of life itself," and seeks to "extrapolate life's purpose from the activities of living organisms" (Luisi 1998). In order to achieve these two goals, Luisi's lab creates minimal cells through the study of self-organization and self-reproduction of chemical and biological systems using compartmentalized reactions (http://www.plluisi.org/). This research supports the hypothesis that cell models synthesized using the proposed system will someday be able to divide, and more closely resemble a natural cell. He is best known for his work with reverse micelles as hosts for various enzymes. Instead of the typical hydrophilic exterior and hydrophobic interior,

reverse micelles consist of the larger, hydrophilic, heads forming in the center due to the presence of a non-polar solvent (figure 4). This creates a polar core, which is able to solubilize water and also enzymes that are much larger than the original core size. Luisi hypothesizes that these reverse micelles may exist in nature, and that they may be suitable models for biological membranes—an essential topic in synthetic biology (Luisi 1985). More recently, Luisi has contributed to the synthetic biology field by attempting to create minimal cells capable of self-assembly and Darwinian evolution in "Synthesizing Life" (Szostak 2001). While minimal cells will be explained further in the next section, they are essentially synthetic cells that contain only the minimum number of components to qualify as a 'living' cell. He writes that in order to meet these criteria, a minimal cell would require a nucleic acid genome and a replicating membrane compartment. For the genome, an RNA replicase is suggested so that it can act "both as a template for storage and transmission of genetic information, and as an RNA polymerase that can replicate its own sequence" (Szostak 2001). Additionally, a simple cell division pattern could be created either by coupling a spontaneous growth mechanism with high environmental shear forces which cause vesicles to divide, or by building the membranes out of lipids with compositions yielding vesicles of "optimum size for thermodynamic stability" (Szostak 2001). This minimal cell prototype can be seen below in figure 3.

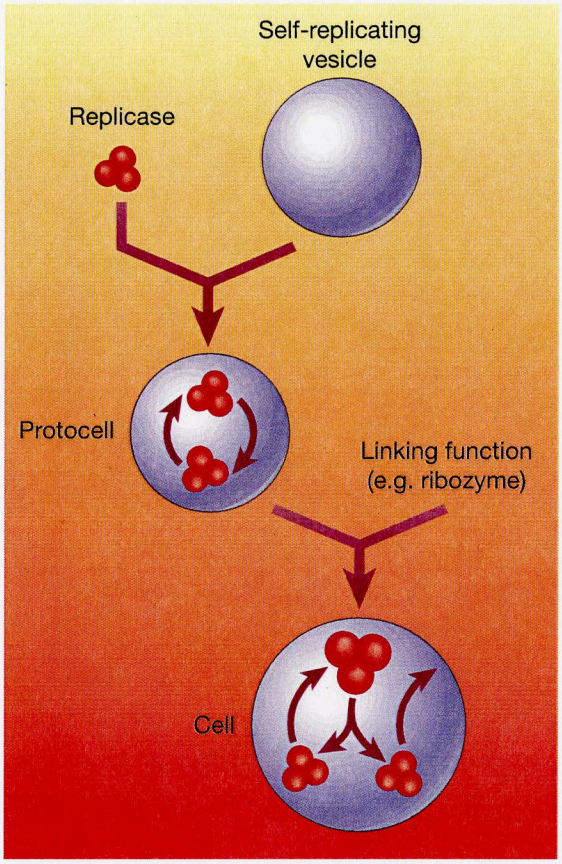

Figure 3. The basic design of Luisi's minimal cell including a self-replicating compartment utilizing the division methods discussed above, and multiple RNA replicases. The two are coupled in order to achieve Darwinian properties (i.e. a ribosome that enables the membrane to grow). (Image from Szostak 2001).

Since molecules can spontaneously become encapsulated in vesicles (although this is not a reliable nor controllable method), Luigi suggests that this simple cell would be simple to synthesize. However, it would not be able to evolve according to Darwinian evolution since the RNA replicase and the membrane would not be coupled unless the RNA-coded activity

resulted in an advantage for the membrane. Further experiments addressing this coupling could result in a population of minimal cells in which evolution is observable, giving insight to early evolution. (Szostak 2001).

Minimal Cells

As mentioned in the discussions of both Luisi and Schwille, the race to create a minimal cell is an instrumental part of the field for bottom-up synthetic biologists. If the smallest functional unit that is still considered to be "alive" is identified, and scientists are able to synthesize a living cell, then it's believed that biological systems will be able to be quantitatively understood and technically mastered (Schwille 2009). This is the ultimate goal of the synthesis of a minimal cell. There are essentially two ways in which synthetic biologists are trying to achieve this. Some are stripping-down all the biological complexities associated with cells and leaving only the essential components to maintain cellular function (Schwille 2011, Schwille 2009). However, previous experiments in which present-day bacteria are stripped down to their minimum essential components still leave hundreds of genes and thousands of different proteins, and so some synthetic biologists have begun to build systems even simpler than bacterium from the ground up—deciding on which components are necessary before synthesis (Szostak 2001). These components are either of biological, organic, or inorganic origins (http://www.biotec.tu-dresden.de/cms/index.php?id=199). As stated previously, the idea of which components are essential is debatable.

Luisi has declared that the essential parts are only the nucleic acid genome and the replicating membrane compartment, while Schwille argues that the essential components are nucleic acids, membrane compartments to encapsulate them, and machinery to transform and replicate these compartments using biological energy (Szostak 2001, Schwille 2009). Although their descriptions are quite similar, Schwille declares a need for separate machinery to facilitate self-replication and evolution, while Luigi claims that this third component is unnecessary. He believes that if RNA instead of DNA is used, then the nucleic acid genome is capable of being both the template for genetic information and the polymerase used to replicate the sequence (Szostak 2001). Scientists such as David Deamer of the University of California-Santa Cruz agree. In "Life After the Synthetic Cell", Deamer goes as far as to say that DNA and proteins can be discarded, and that synthetic RNA can be made to catalyze its own reproduction within an artificial membrane (Deamer 2010). Furthermore, neither Schwille nor Luisi mentioned metabolism machinery while some—including Steen Rasmussen—believe that the metabolism capable of fueling the life process is one of the most important parts of a cell (Rasmussen 2010).

Even after a researcher determines what he or she deems to be the essential parts of a cell, it is then necessary to decide on what constitutes a synthetic cell. If a cell is built using a synthetic membrane, such as a giant unilamellar vesicle, but is encapsulating natural

enzymes and genes, then this can only be considered as semi-synthetic. In order to be truly synthetic, a minimal cell must use a synthetic macromolecular membrane as well as synthetic catalysts and DNA. However, it is thought that a completely synthetic cell is far off in the future (http://www.synbiosafe.eu/index.php?page=synthcells). Debate about the definition of a completely synthetic cell is already occurring, and will be discussed later during the discussion of J. Craig Venter and his synthetic cell.

Typically, liposomes or giant lipid vesicles are used as membrane compartments in the design of minimal cells. This is because they form naturally and can easily encapsulate molecules, such as DNA (Karlsson 2004, Stano 2009, Tsumoto 2001). Most importantly, they possess the ability to self-reproduce—an asset that is essential for a synthetic cell. Furthermore, giant unilamellar vesicles are compatible with optical observation methods such as light and fluorescence microscopy (Schwille 2009). Finally, some scientists have suggested that liposomes may have been precursors to the biological cell, and so they are eager to study the interaction between naturally-occurring cell components with liposome membranes (http://www.synbiosafe.eu/index.php?page=synthcells). However, other types of membranes have been used to model the membranes of a natural cell, including two-dimensional lipid bilayer sheets, micelles, and reverse micelles.

Lipid bilayer sheets have been used by Schwille in order to model membrane-protein interactions in an attempt to characterize the essential components of a minimal cell. In addition to using giant unilamellar lipid vesicles in her research, Schwille also employs a two-dimensional supported membrane system (Schwille 2009). This method involves a polished glass or mica surface with a double layer of lipids forming a unilamellar membrane on top of it (Schwille 2009). Using the two-dimensional model is more effective for studying the transport of particles through the membrane due to its ability to be observed using optical microscopy and spectroscopy, and makes this process more accurate by forming a thin hydration layer beneath the membrane that allows for lipids to move more freely and does not allow the lipids to be affected by the supportive surface (Schwille 2009). Furthermore, these supported membranes offer the opportunity for the researcher to model asymmetric bilayers, which more closely resemble natural membranes (Schwille 2009).

As mentioned previously, Luisi has used reverse micelles in place of the standard liposomes in his minimal cell systems. Reverse micelles are supramolecular structures that form spontaneously when surfactants are dispersed in an apolar phase in the presence of a small amount of aqueous phase (Stano 2010). Since they encapsulate the aqueous (polar) phase, they are able to host large water-soluble macromolecules within their dynamic membranes, including long DNA molecules or even plasmids (Luisi 2008). Reverse micelles are also good membranes to use for synthesizing cell models because a large

number can be made to each encapsulate the same amount of material. This is because they rapidly exchange their content, which leads to equal concentrations within the reverse micelle population (Luisi 2008). Similar to liposomes, reverse micelles also self-reproduce, making them an effective choice for minimal cell membranes (Stano 2010). Micelles are also used frequently, most notable in a minimal cell system developed by Steen Rasmussen (Stano 2010). These various compartments used for the encapsulation of molecules in the design of synthetic cells can be seen below in figure 4.

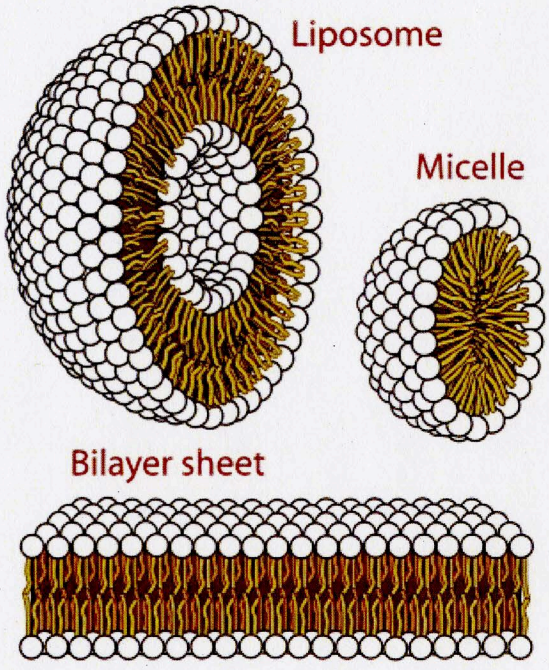

Figure 4. A liposome, a micelle, and a lipid bilayer sheet. The white spheres represent the hydrophilic heads, while the orange lines represent the hydrophobic tails. Reverse micelles are simply micelles with the hydrophilic heads on the inside and the hydrophobic tails on the outside, in a nonpolar solvent. (Image from http://www.pharmainfo.net/reviews/overview-brain-targeting-drug-delivery-system).

David Deamer claims that minimal cells, especially those with a synthetic RNA acting as a catalyst and genetic molecule and an artificial membrane, could represent the first cells on Earth from nearly four billion years ago (Deamer 2010). Thus, if a simple system is designed and is able to self-reproduce and evolve in a Darwinian manner, scientists may be closer to understanding the origins of life, and these necessary cell components may represent the essential properties of life (Szostak 2001). Knowledge of the "essential properties of life" would surely allow synthetic biologists to design completely synthetic systems capable of displaying attributes of their choosing. The completion of a completely synthetic minimal cell would prove that life can be arising from non-living components, which brings up a much bigger issue—where do you draw the line between dead and living matter? (http://www.biotec.tu-dresden.de/cms/index.php?id=199). Finally, completely synthetic cells could be mass produced and made to operate in a specific manner so that they would be beneficial for use as microcompartment bioreactors, or drug delivery vesicles (http://www.synbiosafe.eu/indec.php?page=synthcells).

Top-Down Synthetic Biology

Perhaps the most work has been done in the second direction of the field. Synthetic biologists have jumped at the opportunity to modify natural cells to do their bidding. A popular analogy in the field is to think of these "rewired" cells as cellular circuits. Synthetic biologists are using naturally occurring components to essentially design circuits with the

ability to time events (Ellis 2009), toggle between gene expression (Gardner 2000), oscillate between activators and repressors (Atkinson 2003), detect light and dark regions in an image of light (Tabor 2009), play tic-tac-toe (Stojanovic 2003), and produce insulin (Goeddel 1979). A few distinguished synthetic biologists who utilize the top-down method are Steven A. Benner, George Church, J. Craig Venter, and Jay Keasling.

Steven A. Benner conducted his research at the University of Florida until 2005, when he founded the Westheimer Institute of Science and Technology (TWIST) and the Foundation for Applied Molecular Evolution (FfAME). His research group was the first to synthesize a gene for an enzyme, according to his FfAME website, and has prepared the "first artificial genetic systems," which are being used in "FDA-approved clinical assays for HIV, hepatitis B and hepatitis C." Like many bottom-up synthetic biologists, his team focuses on the ability of unnatural cells to self-sustain and undergo Darwinian evolution (http://ffame.org/sbenner.php). One significant example of Benner's work is his well-known article "Exhaustive matching of the entire protein-sequence database", where his team developed methods to be used to "manage sequence data generated by major genome sequencing projects", specifically, the human genome project (Gonnet 1992). With regards to synthetic biology, Benner and his research associates have contributed mostly by developing an artificial genetic system by the incorporation of new complementary Watson-Crick base pairs κ and X (as well as its analogue π) into both RNA and DNA. These

new base pairs can be seen below along with the natural pairs cytosine-guanine and adenine-thymine/uracil, in figure 5 below.

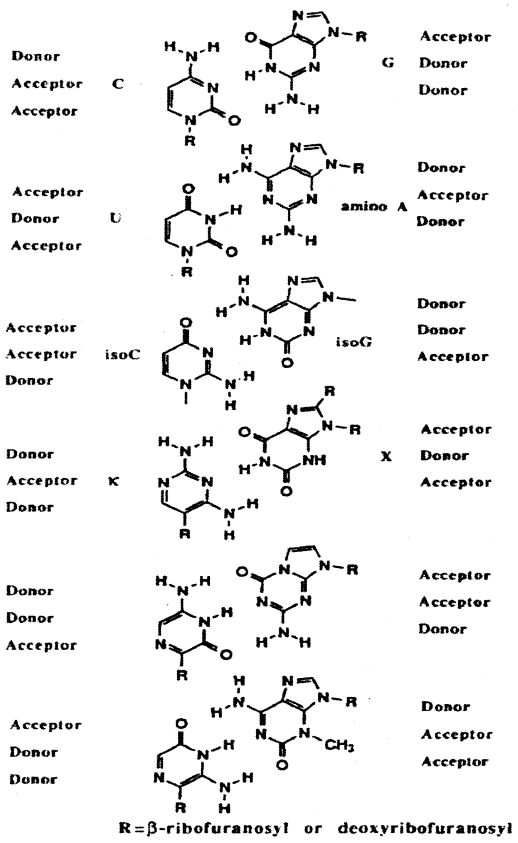

Figure 5. Independently replicable base pairs. Each base pair shown has an individual and mutually exclusive hydrogen-bonding pattern and is capable of forming Watson-Crick base pairs with three hydrogen bonds. In the top image, the cytosine and guanine base pair is shown. In the second, the adenine and uracil base pair is shown. In the third image, the experimental base pair iso-cytosine and iso-guanine is shown, although it was discovered to not be ideal. In the fourth image, the synthetic base pair κ, or 3-β-D-ribofuranosyl-(2,6-diaminopyrimidine), and X, or xanthosine, is shown. In this article, π, or 7-methyl oxoformycin B, was used in place of X due to concerns regarding X depurination. The last two images are two other mutually exclusive hydrogen-bonding schemes, which were not addressed. (Image from Piccirilli 1990).

The availability of a new base pair could mean an expanded genetic code and therefore a larger number of amino acids able to be incorporated into proteins (Piccirilli 1990). This would be a significant step for the synthetic biology field, allowing for researchers to develop cells with partially synthetic genomes capable of producing a vast array of proteins in order to produce new materials with desirable properties. Additionally, if these unnatural amino acids are able to be synthesized through cell division, these polymers would be able to be reproduced more precisely than if reproduced in a lab.

George Church is a professor of Genetics at Harvard Medical School, a core faculty member at Harvard's Wyss Institute for Biologically Inspired Engineering, and focuses mostly on the synthesis of personal genomic systems and biofuels. (http://www.hms.harvard.edu/dms/BBS/fac/church.php). He achieved fame before his work as a synthetic biologist by helping initiate the Human Genome Project after developing the first direct genomic sequencing method in 1984 (Church 1984). One prominent example of his research in synthetic biology is his work done with James Collins to synthesize a gene network with the ability to count. The idea for this originated when it was noted that natural phenotypic changes appeared to be the result of the system reaching some critical density, implying that the natural system utilized a naturally occurring counting mechanism. To replicate this phenomenon, their team developed a riboregulated transcriptional cascade counter to be used with two transcriptional cascades in E. coli. The first allowed the cell to "count" to two by expressing various proteins (T7

RNAP and GFP) in response to either the first or second arabinose pulse. The second allowed the cell to "count" to three using the same system but one more cascade node, and released T7 RNAP, T3 RNAP, and GFP after the first, second, and third pulses respectively. These mechanisms and results can be seen in figure 6, below.

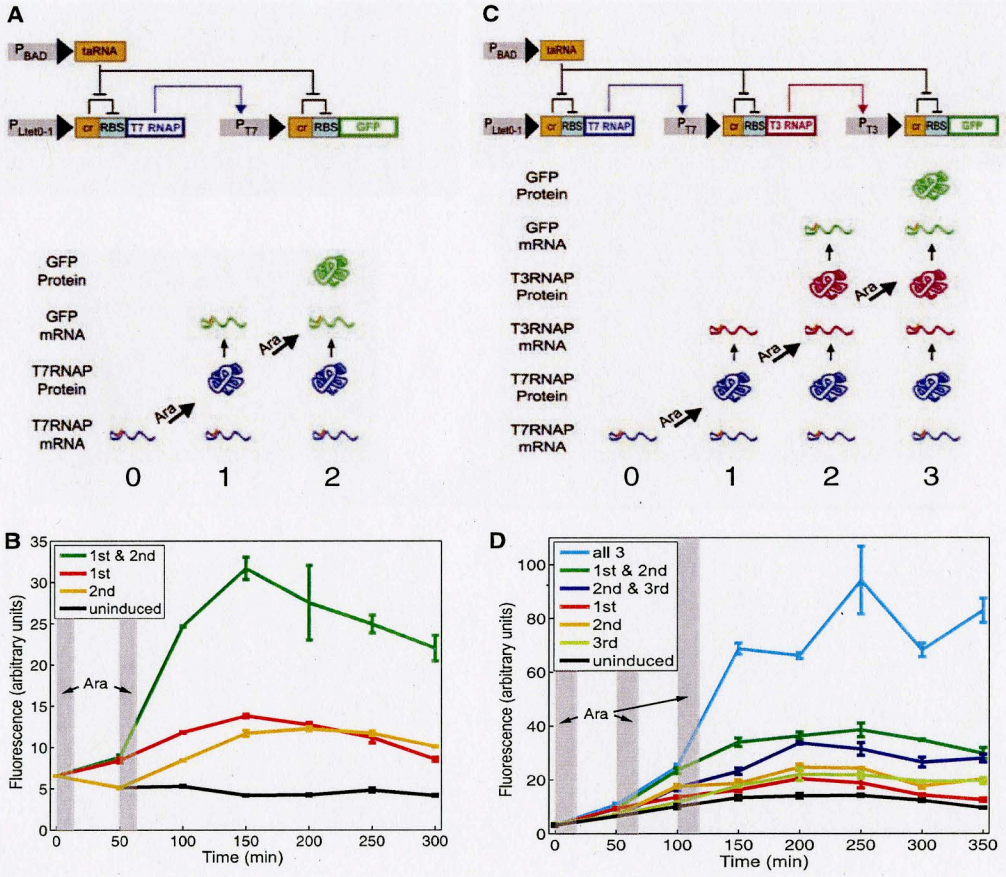

Figure 6. Images A and C show the transcriptional cascades used by the two-counter system, and the three-counter system, respectively. Image B shows the fluorescence (as observed due to the presence of GFP) measured in four separate counter cells over time. The first was only given the first pulse, the second, only the second pulse, the third received both, and the fourth was given no pulses. Image D shows a similar experiment done with the three-counter system and seven separate cells. (Image from Friedland 2009).

Although this system can be seen as a valuable modular addition to any cellular circuit, problems still include low responses to imperfect pulse lengths and frequencies. However, if this technology were developed further, the authors suggest that the counter could be used to program cell death after a certain number of cell divisions. (Friedland 2009).

J. Craig Venter worked at the NIH and at the State University of New York at Buffalo before founding the J. Craig Venter Institute in 2006 where he is currently working as the president. In 2005, he founded Synthetic Genomics, a company focused on producing biofuels while collaborating with ExxonMobil. (http://www.jcvi.org/cms/about/overview/). Similarly to Benner and Church, Venter also achieved fame for his role in sequencing the human genome. His most famous article—entitled "The sequence of the human genome"—features Venter as the first author along with Francis Collins of the National Institutes of Health and over one hundred other researches who generated a "2.91-billion base pair (bp) consensus sequence of the euchromatic portion of the human genome by the whole-genome shotgun sequencing method" (Venter 2001). In the synthetic biology world, he gained notoriety once again for creating the first cell with an entirely synthetic genome in 2010—a feat that triggered much debate in the synthetic biology field. Venter's team began by sequencing and synthesizing the *Mycoplasma genitalium* bacterium genome in 1995, and later did the same for the faster-growing and therefore more ideal bacterium *Mycoplasma mycoides*. This 1.08-mega-base pair synthetic genome was grown as a yeast centromeric plasmid, cloned,

extracted, methylated, and transplanted into a *Mycoplasma capricolum* recipient bacterium. (Gibson 2010). An image of the synthetic Mycoplasma mycoides genome can be seen below in figure 7 below.

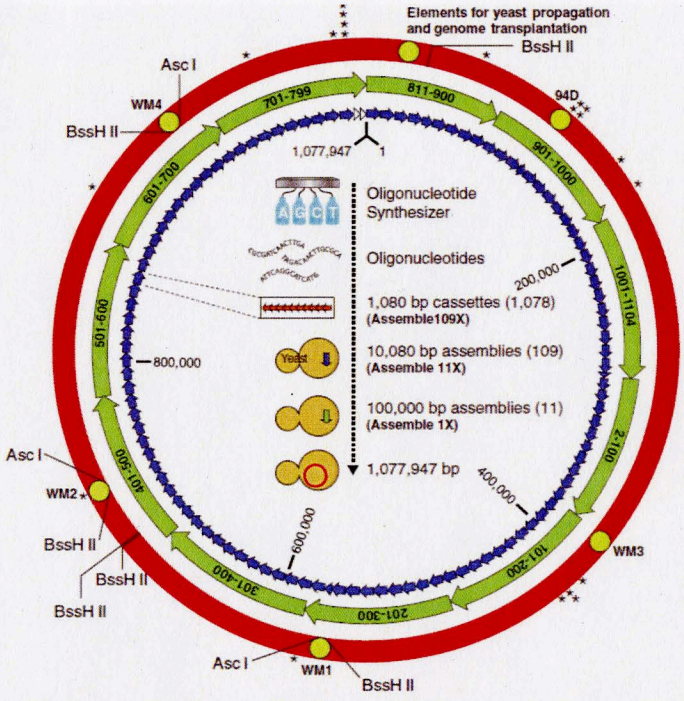

Figure 7. The 1078 DNA cassettes of the synthetic genome. The orange arrows represent the 1080-bp cassettes made of synthetic oligonucleotides which were recombined in sets of ten to produce 109 ~10-kb assemblies, which are represented by the blue arrows. (While most of these were created via in vivo homologous recombination in yeast, the two white arrows represent the two constructs that were enzymatically pieced together in vitro.) These were then recombined in sets of ten to produce 109 ~100-kb assemblies which are represented by the green arrows. These were then recombined into the complete genome, which is represented by the red circle. (Image from Gibson 2010).

As Venter's team states in the report, "we refer to such a cell controlled by a genome assembled from chemically synthesized pieces of DNA as a synthetic cell, even though the

cytoplasm of the recipient cell is not synthetic" (Gibson 2010). As previously stated, this sparked discussion among researchers in the field who claimed that simply synthesizing a genome does not mean that the cell is entirely synthetic, especially when introduced to biologists working on the synthesis of minimal cells. George Church stated that "printing out a copy of an ancient text isn't the same as understanding the language...the grand challenge remains understanding the parts of cells that help the DNA to function" ("Life After the Synthetic Cell" 2010). However, Venter's team disputed this claim by stating that "the properties of the cells controlled by the assembled genome are expected to be the same as if the whole cell had been produced synthetically (the DNA software builds its own hardware)" (Gibson 2010). As this research can be seen as one of the most advanced projects in synthetic biology, it also caused much ethical debate, raising philosophical issues regarding the synthesis of new life, which will be discussed later.

Jay Keasling is a professor of Chemical and Biomolecular Engineering and Bioengineering at the University of California, Berkeley. Keasling works on many synthetic biology projects involving the metabolic engineering of microogranisms with a final goal of developing tools to allow precise and reproducible control of metabolism (http://cheme.berkeley.edu/faculty/keasling/). He hopes to be able to apply these tools to the synthesis of biodegradable polymers, the accumulation of phosphate and heavy metals and the degradation of chlorinated and aromatic hydrocarbons, the biodesulfurization of fossil fuels, and the complete mineralization of organophosphate nerve agents and

pesticides (http://cheme.berkeley.edu/faculty/keasling/). One of his most cited works is an article in which Keasling and J. Pramanik develop a stoichiometric model with 153 reversible and 147 irreversible reactions to describe the steady-state growth of Escherichia coli on glucose and mineral salts (Pramanik 1997). This work is significant because it describes the overall flux distribution in the bacterium, and can help determine how this will be determined if the bacterium is used to synthesize a product or degrade a pollutant. Most recently, Keasling has impacted the synthetic biology field by engineering Saccharomyces cerevisiae yeast to produce artemisinic acid, which is the precursor to artemisinin—a drug used to treat malaria (Ro 2006). Essentially, the yeast cells were engineered to express the enzyme amorphadiene synthase and a cytochrome P450 monooxygenase. A more detailed look at the process can be seen below in figure 8.

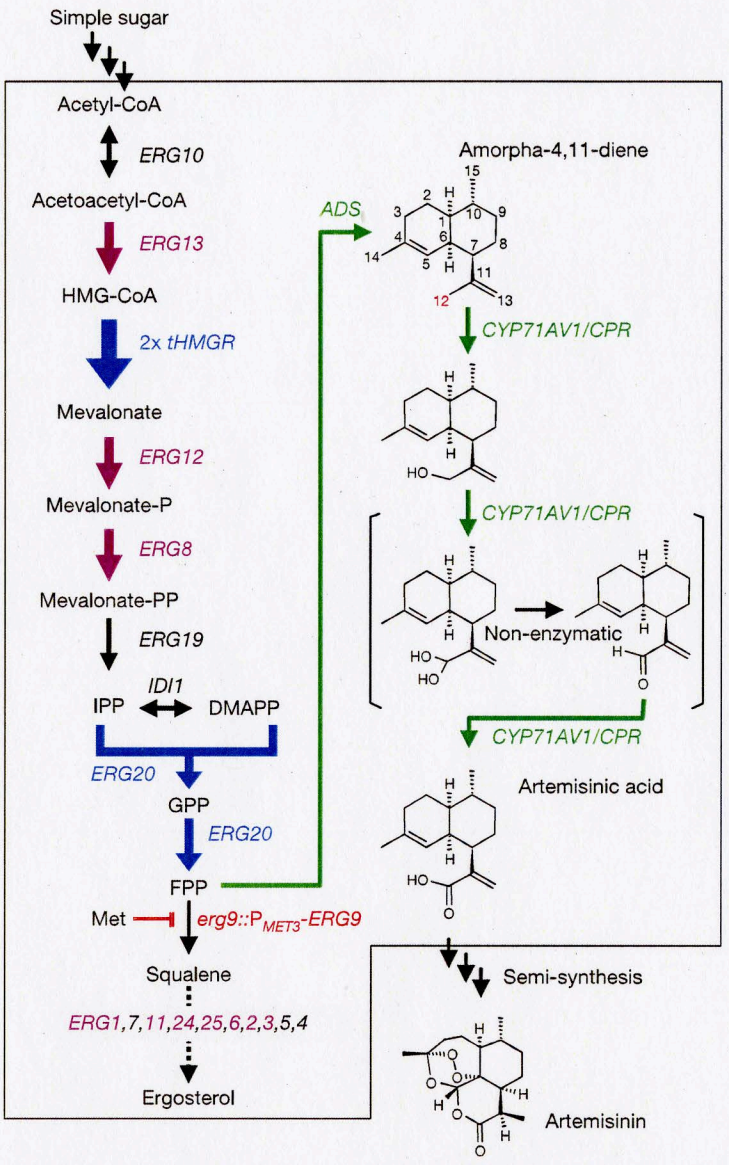

Figure 8. A schematic representation of the biosynthetic pathway expressing CYP71AV1. The blue arrows represent genes from the mevalonate pathway that are directly upregulated. The purple arrows represent genes that are indirectly upregulated by upc2-1 expression. The green arrows represent the biochemical pathway leading from FPP to artemisinic acid, which was introduced from A. annua. Also, the three oxidation steps converting amorphadiene to artemisinic acid by CYP71AV1 and CPR are shown. The red line represents the repression of ERG9. (Image from Ro 2006).

This is a project funded by the Bill and Melinda Gates Foundation and has resulted in a dramatic decrease in cost for each artemisinin dose—from $2.40 to $0.25 (Ro 2006). Keasling claims that the semisynthetic artemisinin from engineered yeast will become available in 2012, and that it will assist in the fight against malaria, particularly in Africa.

Timeline

The following timeline (figure 9) indicates some substantial milestones achieved in the synthetic biology field. It is difficult to define the beginning of synthetic biology history, since the definition of synthetic biology itself is not universally agreed upon. For example, the first mention of synthetic biology was in the 1980, although many do not consider the term to apply today as it did back then (Benner 2005). Furthermore, some consider the re-engineering of biological systems to be biomedical engineering today, instead of what was once known as synthetic biology.

The timeline may seem bare when considering that it encompasses an entire field, but this is due to the constraints that synthetic biologists face. These include the vast number of undefined and complex biological parts, the unpredictability and unwieldiness of these parts, the fact that many of these parts are incompatible with each other, and the unreliability of these parts over time (Kwok 2010). While keeping the daunting nature of this field in mind, this timeline should be thought of as a "modern synthetic biology"

history, since it only goes back to the year 2000. It should also be noted that some major events, such as the construction of Venter's "synthetic cell" have occurred more recently and are not featured on the timeline.

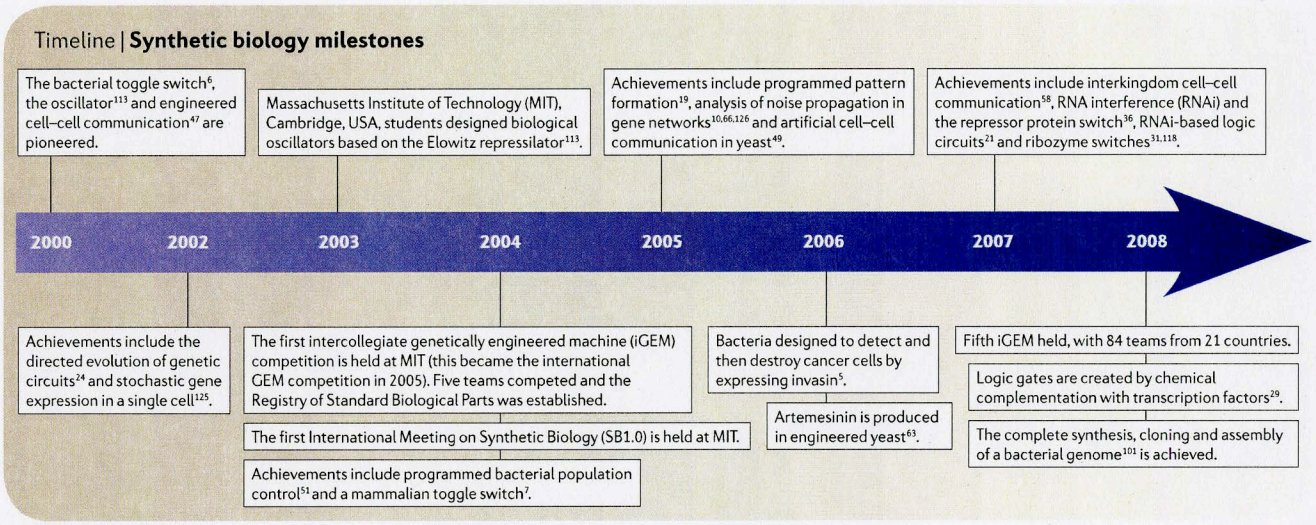

Figure 9. Timeline featuring important milestones in the synthetic biology field. (Image from Purnick 2009)

3. Current Applications of Liposomes

As mentioned during the previous discussion of minimal cells, liposomes have an important role in synthetic biology, and are typically used as membrane compartments for synthetic cells. While this use will be discussed further, it is also important to note the application of liposomes by biologists and biomedical engineers as both transport vesicles and reaction vesicles. It is thought that the following three applications of liposomes are the most performed today, although not necessarily in the field of synthetic biology.

Researchers who use these methods in their work will likely be able to apply these processes utilizing liposomes towards the study of synthetic biology.

Liposomes as Synthetic Cell Membranes

As discussed previously, liposomes are the membrane of choice for most researchers working on synthetic cells. This is mainly because liposomes are self-assembled from phospholipid monomer dispersions into vesicles due to their lipid membrane properties and their surface properties greatly resemble those of a natural cell membrane. In order to more closely resemble natural cell membranes (in which lipids only comprise less than 50% of the membrane, while the rest is comprised of membrane proteins and channels), synthetic biologists have inserted functional membrane proteins into lipid bilayers. One of the first examples of this is in the work done by David O'Brien, in which the G-protein-coupled receptor rhodopsin was reconstituted in phospholipid bilayer membranes, and its absorption effects were observed (O'Brien 1977). Another example, as mentioned in the discussion of Petra Schwille, involves the attachment of natural elements such as filamentous actin to the lipid membrane to maintain the shape of the liposome and even more-so make the lipid membrane resemble the structure and functionality of that in natural cells. An example of this can be seen below, in figure 10.

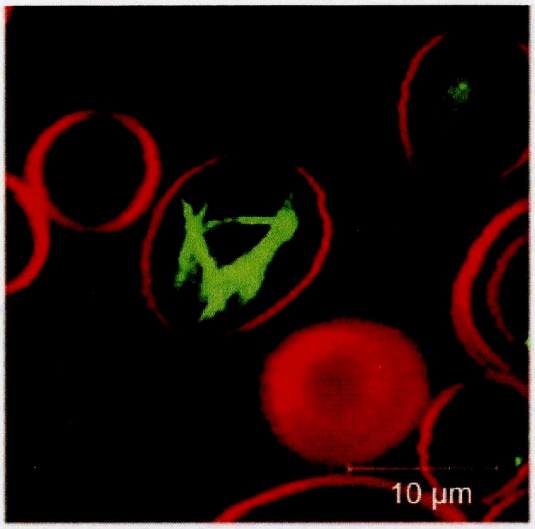

Figure 10. A giant unilamellar vesicle can be seen in red using lipid dye DiD C18, while the red spectrin-ankyrin system can be seen in green using phalloidin-Alexa 488 conjugate dye. This is a completely synthetic cell, which is beginning to resemble a natural cell, although is still lacking most elements including genetics (Image from Merkle 2008).

There are a variety of liposomes that can be used as membranes for synthetic cells. These can be abbreviated with three letters, such as GUV for the aforementioned giant unilamellar vesicle. The first letter represents the size of the vesicle, and can be either "S" if the vesicle is small (under 50 nm), "L" if the vesicle is large (about 100 nm), or "G" if the vesicle is giant (about 1 micron). The most stable of these sizes is thought to be the large vesicle, while the only one that can be seen using a standard microscope is the giant vesicle. The second letter represents the number of layers—lipid bilayers in the case of liposomes. A "U" represents a unilamellar vesicle, meaning that the vesicle contains only one lipid bilayer, thus the standard liposome. An "M" represents a multilamellar vesicle, and finally, a "P" represents a polylamellar vesicle. The third letter, "V", simply stands for vesicle. The

liposomes most commonly used for synthetic cell membranes are GUV's, while LUV's are often used for other tasks such as drug delivery or as reaction vesicles.

Liposomes as Transport Vesicles

Perhaps the biggest use of liposomes in the fields of biology and biomedical engineering is for transport vesicles inside the human body—particularly in drug delivery systems. Liposomes make good transport vesicles because of their aforementioned encapsulation properties and the ease associated with their synthesis. They can carry both hydrophobic and hydrophilic molecules, since they can be made to encapsulate hydrophilic molecules within the center of the liposome, and can store hydrophobic molecules within the membrane (http://www.news-medical.net/health/Liposome-Uses.aspx). Since hydrophilic molecules will not diffuse through the liposome lipid bilayer, and hydrophobic molecules will not diffuse out of the membrane, they will be maintained inside the vesicle until they are somehow released—typically through either fusion, diffusion, or endocytosis. The most basic method of delivery is through the fusion with other bilayers, such as natural cell membranes. Once the liposome fuses to an endothelial cell, or some other type of cell membrane, it can naturally release its contents, provided that the membrane composition was designed to facilitate release and that the content is not destroyed in the host cell's lysosomes (http://www.news-medical.net/health/Liposome-Uses.aspx). Another method of delivery is diffusion, in which charged particles are utilized to trigger the release of molecules. Encapsulated solutions can be made to be at a certain pH so that the

encapsulated aqueous drugs are initially charged within the liposome, and unable to pass through the non-polar membrane (http://www.news-medical.net/health/Liposome-Uses.aspx). Over time, the solution will neutralize as protons pass freely through the membrane, resulting in the encapsulated drugs returning to their neutralized pH, and being able to pass freely through the lipid bilayer (http://www.news-medical.net/health/Liposome-Uses.aspx). Finally, the last basic method is through the use of endocytosis. If the liposome is synthesized to be large enough, it will be a natural target of the body's macrophages for phagocytosis—or the natural destruction and elimination of the liposome (http://www.news-medical.net/health/Liposome-Uses.aspx). This process will release the drugs encapsulated by the destroyed liposome vesicle.

All of the above methods can be used to distribute a variety of molecules in vivo. Some of these include the delivery of microbubble contrast agents used in certain methods of contrast-enhanced ultrasound imaging (Turkbey 2009), the delivery of DNA into a host cell, the delivery of pesticides to plants (Meure 2009), the delivery of enzymes and nutritional supplements to food (Meure 2009), the delivery of cosmetics to the skin (Meure 2009), the delivery of dyes to textiles (Barani 2008), and the delivery of drugs—particularly chemotherapeutic drugs.

Liposomes are particularly useful for the delivery of chemotherapeutic drugs because they are able to target tumors by utilizing 'leaky" blood vessels created rapidly through tumor angiogenesis. This targeting is made possible due to the fact that endothelial cells in normal blood vessels are bound together by tight junctions, preventing large particles in the blood from leaving the vessel (Turkbey 2009). However, when tumors begin to rapidly grow, they need a rapidly growing blood supply, and so they undergo a very rapid angiogenesis, resulting in the lack of tight junctions and the presence of "leaky" vessels surrounding the tumor site in which particles under about 200 nm can travel through (Turkbey 2009). This allows for drug delivery vesicles to travel through the blood stream without exiting the blood vessels until they reach the tumor site and are able to leave through the leaky vessels. This application is especially appropriate for liposomes that are close to 100 nm in diameter, which is the size that they are made to be in the Romanowski lab (Yuan 1995). It is especially useful for drug delivery systems carrying chemotherapeutic drugs to be targeting because of the numerous adverse effects on healthy tissue that is caused by those drugs.

In order to further ensure specific targeting, liposomes that are employed as drug transport vesicles are typically made with the addition of ligands, which will activate endocytosis only in specific cell types or only in the presence of unhealthy tissues. Certain ligands are known to bind to certain proteins, so researchers can choose the ligands that bind to the proteins that are known to be present at various tumor sites. One example is the

protein CD40, which is expressed by the tumor during the late stages of ovarian cancer and can be targeted using CD40-targeting ligand-coated liposomes encapsulating drugs that induce apoptosis within the tumor, and theoretically, *only* in the tumor (Jiang 2008). Chemotherapeutic drugs are most often associated with the use of liposomes and ligands in drug delivery research as many researchers attempt to minimize the negative effects of chemotherapeutic drugs on other cells that naturally divide rapidly, such as cells in the bone marrow, digestive tract, and hair follicles. Finally, liposomes used in drug delivery are also often PEGylated, meaning that they are often coated in hydrophilic polyethylene glycol chains, which help space out liposomes in a solution, and help to mask the liposome from the body's immune system so that it can circulate within the blood stream for a longer period of time in order to reach its destination (http://www.sciencedaily.com/releases/2010/03/100311101612.htm). An illustration of a liposome used for drug delivery can be seen below in figure 11.

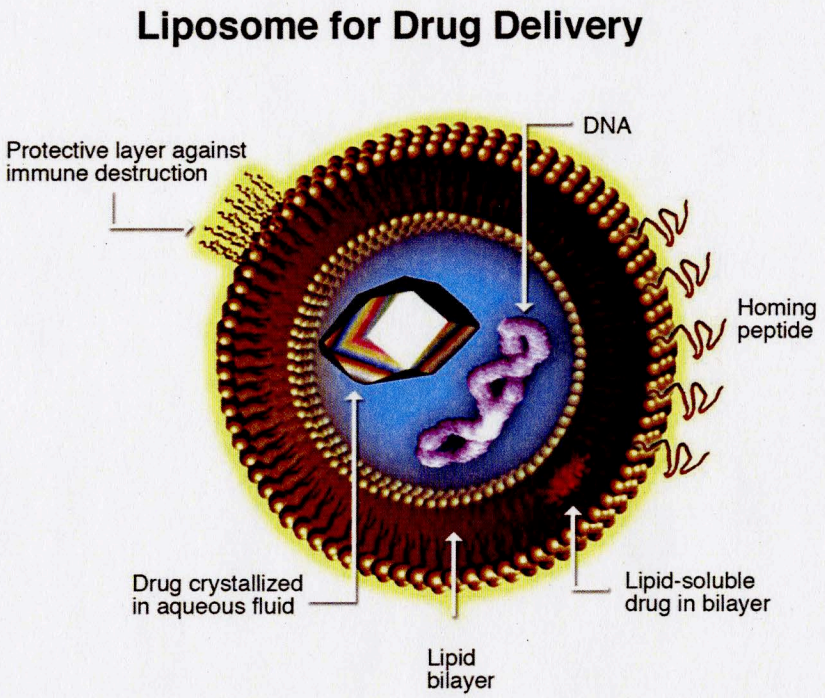

Figure 11. A depiction of a liposome used for drug delivery. The lipid bilayer can be seen with a hydrophilic interior and exterior and a hydrophobic membrane. An aqueous drug can be seen encapsulated within the liposome and a homing peptide, which completes the same tasks as a ligand, can be seen on the outside of the lipid bilayer. Finally, the protective layer against immune destruction is a series of PEG chains covalently bonded to the liposome during the PEGylation process. (Image from http://en.wikipedia.org/wiki/File:Liposome.jpg)

Although drug delivery is an especially studied application of liposomes today, in vitro applications are also just as important, especially with regard to the potential synthesis of a minimal cell, and the transport of material within that minimal cell or within natural cells. A possible in vitro application for liposomes as transport vesicles in the field of synthetic biology will be discussed later.

Liposomes as Reaction Vessels

Many researchers hoping to observe mixing and transport phenomena properties on a small, cellular scale have began to turn to liposomes as reaction vessels instead of the standard lab equipment. Previously, all in vitro experiments were carried out in large "hard" vessels (glass or plastic apparatuses at 1-100 millimeters in diameter), which did not represent how they are carried out in life, which is within smaller "soft" compartments (closed biomembranes at 0.1-10 microns in diameter) (Tsumoto 2001). In order to more closely model the natural chemical reactions occurring in cells, some researchers have begun to use liposomes as reaction vessels, since they much more closely resemble natural cells than do test tubes or petri dishes. This is an important advancement in the biology and biomedical engineering fields because small scale systems are dominated by surface interactions, making the negative impacts of hard surfaces even more noticeable on the cellular level, and making the surface properties of the containment vessels of utmost importance. According to Mattias Karlsson in a review of nanoscale reactors, the materials used to create reaction vessels should offer the ability to control "wettability, charge, specific binding interactions and other interactions that have a bearing on water structure, solvation, depletion interactions, and many more phenomena," and lipid bilayers are the best living systems which adhere to these guidelines (Karlsson 2004). The easily-manipulated surface properties that liposomes possess make them a clear choice for reaction vessels, and allow for the elimination of the adverse surface effects of solid

surfaces with the chemical reactions, especially as the surface area to volume ratio increases when reactions are performed on a smaller, cellular, scale (Tsumoto 2001).

In addition to a better resemblance of a natural cell membrane, liposomes serve as good reaction vessels because of their size. When researchers want to recreate or study the chemical reactions that take place naturally within a cellular environment, it makes much more sense to do so on a cellular scale. Liposomes are able to mimic the reactions that take place in biological systems on a nanometer-length scale, making it possible to carry-out reactions that rely on extremely small sample volumes. (Karlsson 2004). Additionally, it is useful to develop a technique for performing chemistry with controlled reaction initiation, mixing, and mass transport in nanoscale devices with few molecules because of the recent focus on nanotechnology (Karlsson 2004). Liposomes are the most suitable for this purpose because they can contain controlled chemical reactions in confined biomimetic compartments (Karlsson 2004). Additionally, these small, individual vesicles can be made in different sizes and to correlate the reaction kinetics with theoretical models in order to investigate the effect of compartmentalization on spatial and temporal correlation among reactants in these systems (Karlsson 2004). An experiment such as this could not be done using the standard lab equipment due to size restraints and a significant lacking in size variability. Furthermore, using liposomes as reaction vessels is a way to downsize the scale of laboratory experiments, and therefore the cost (Tsumoto 2001).

Another benefit of using liposomes as reaction vessels is the ability to control both the interior and exterior media in the same way that a synthetic membrane would, but with the ability to more closely mimic natural cellular membranes. Membrane chemistry can also take place within a liposome, as seen in the work by Petra Schwille in which membrane proteins were added to a liposome and were shown to function in the same way as they would in a natural cell. The membrane benefit of a liposome compared to standard glass lab equipment can be seen below in figure 12.

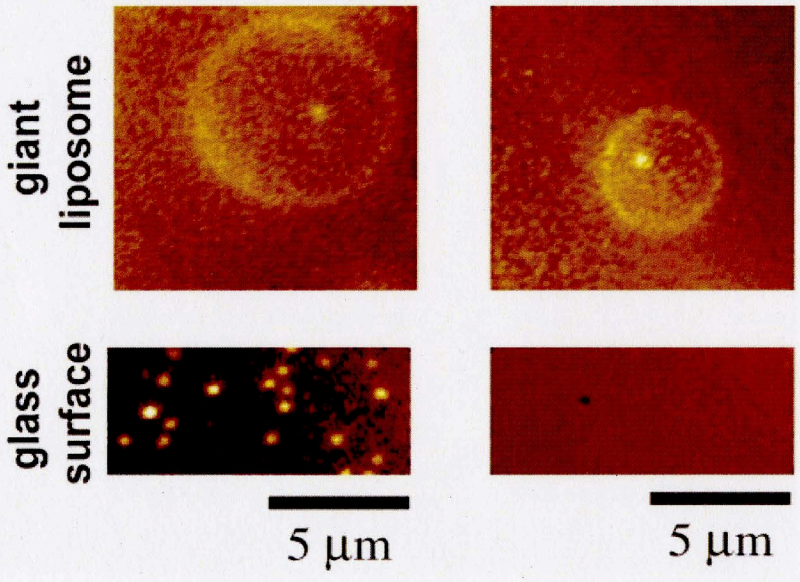

Figure 12. Shown here is a giant liposome encapsulating a biochemical reaction, and protecting the reaction products from the enzyme outside. The two images on the left are without the presence of RNase, while the two on the right are in the presence of RNase. It can be seen that the RNA inside the liposome is still present in the presence of RNase, while the RNA adsorbed onto a glass surface has been degraded in the presence of RNase. (Image from Tsumoto 2001)

The use of lipid vesicles to model transport phenomena properties interests researchers because it helps them to understand how chemical reactions proceed in terms of kinetics and transport mechanisms in a small-scale environment. Studying chemical reactions and molecular or colloidal behaviors such as single-file diffusion or transport in confined and biomimetic geometries with tailored surface properties and well-defined internal and external media is possible with liposomes, when it has never been plausible before (Karlsson 2004). Solitary liposomes are powerful for initiating reactions in single micron-diameter containers and can be used to create cellular models for mapping signaling pathways and intracellular transport phenomena where the complexity can be increased at will by the researcher (Karlsson 2004). All of these aspects have resulted in the increased use of liposomes as reaction vessels in recent times.

4. Relevant Techniques Currently Used in the Lab

Current research in the lab revolves around the coating of loaded liposomes with gold nanoparticles, and maneuvering and unloading them through the use of an optical trap. This section will discuss the processes currently being utilized in the lab including optical trapping, the current optical trapping and microscope set-up, and light-responsive liposomes.

Optical Trapping

Optical traps are tightly focused laser beams formed by an objective lens with a high numerical aperture that are used to control the three-dimensional movement of particles within the beam's path, as long as the beam has a Gaussian intensity profile (Neuman 2004). The scattering of incident photons due to the beam results in a net momentum transfer to the dielectric particle, which can be described using two forces: a scattering force in the direction of light propagation and a gradient force in the direction of the spatial light gradient, with the gradient force dominating (Neuman 2004). The scattering force is due to the firing of photons in the direction of the particle, and takes absorption into account. It results in movement in the forward direction only since the scattering forces cancel out in every other direction (Neuman 2004). The gradient force is due to the particle, which is a fluctuating dipole, existing in an inhomogeneous electric field, and is entirely in the direction of the field gradient (Neuman 2004). A depiction of these forces can be seen below in figure 13.

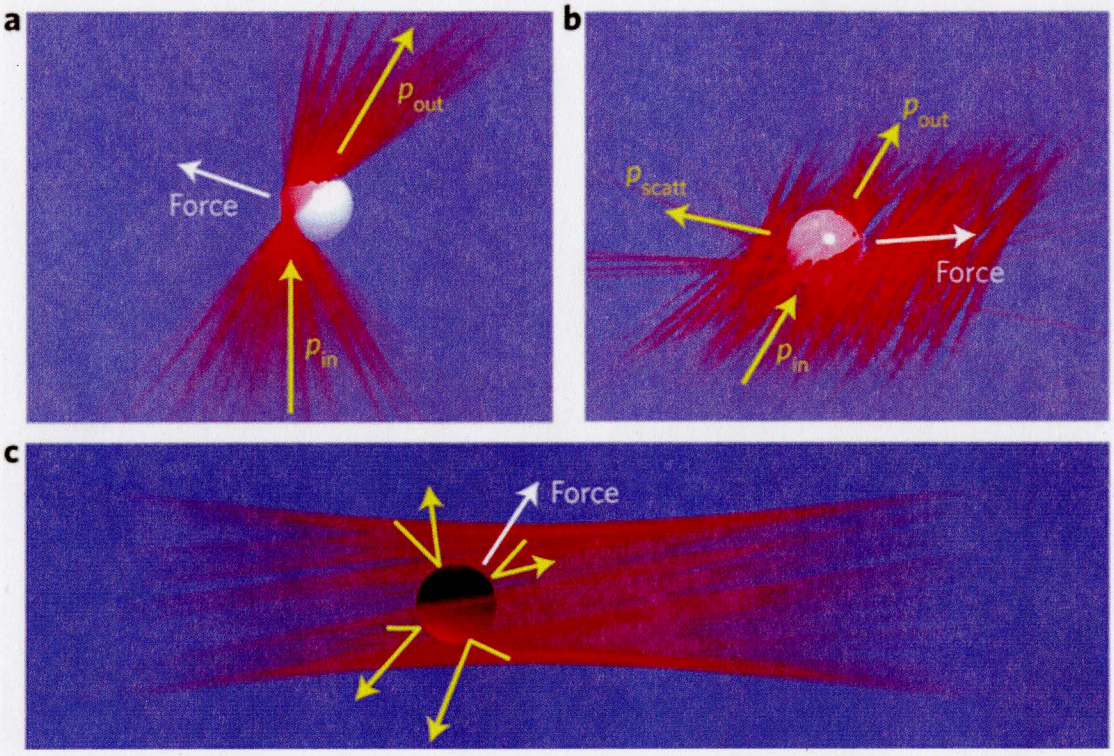

Figure 13. Image A shows the gradient force, in which a refractive particle moves towards the brightest point of the beam where p_{in} and p_{out} are the momentum of the incident light and of the refracted light, respectively. Image B shows the reflected light pushing the particle in the direction of the Poynting vector, which is the scattering force. Image C shows the absorbing particle being heated, creating a thermal gradient across the surface that may create unwanted forces, preventing the formation of a stable trap. The sum of these three forces result in a force that can levitate, trap and transport particles (Image from Padgett 2011).

Originally developed in the 1970's, optical traps have since been used heavily in the field of biomedical engineering, particularly in the study of molecular motors, the physics of colloids and mesoscopic systems, and the mechanical properties of polymers and biopolymers (Neuman 2004). The standard, basic optical trap is built in the lab using an inverted microscope with beam steering and amplitude modulation elements introduced

into the optical path before the objective lens; position detecting elements are usually also included (Neuman 2004). Commercial, motorized systems can also be used, and will be discussed later. A diagram of a basic optical trap design can be seen below, in figure 14.

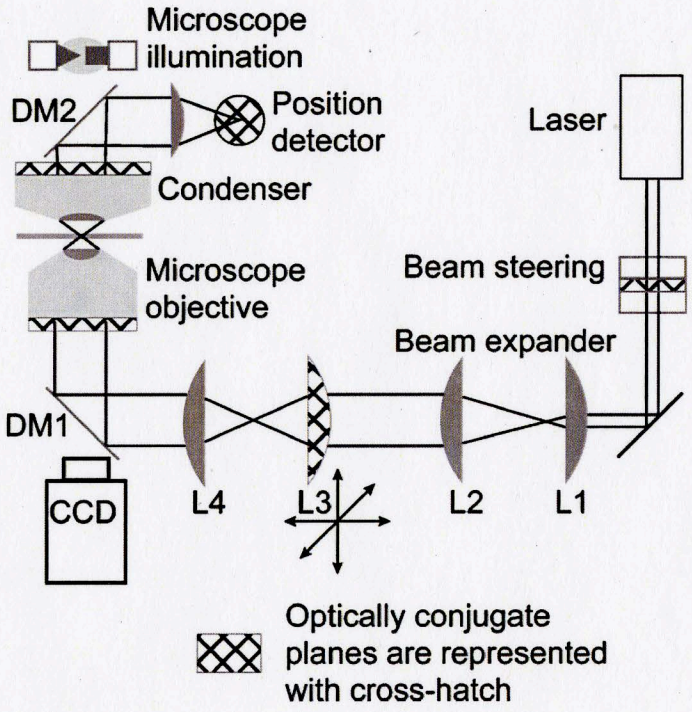

Figure 14. Layout of a generic optical trap. The beam begins in the top right, where it is steered using a beam steering device. It then goes through the beam expander (L1 and L2, which are typically a Keplerian telescope) so that it will be large enough to overfill the back aperture of the objective. Next, the beam will go through lenses 3 and 4, which change the divergence of the light entering the objective and the axial location of the laser focus. From there, the laser is coupled into the objective lens by a dichroic mirror (DM1), which "reflects the laser wavelength, while transmitting the illumination wavelength"(Neuman 2004). The actual optical trap is created when the laser beam is brought back into focus by the objective lens. Forward scattered light is collected by the condenser and coupled onto the position detector using DM2. A trap steering system can also be implemented in a conjugate plane to the objective back aperture. The CCD, or charged couple device, is a grid sensor that is used for capturing images of the trapped object (Image from Neuman 2004).

Currently in the lab, a laser set-up similar to the one above is used both to guide liposomes coated with gold nanoparticles to desired locations and release the content within the liposomes.

Current Optical Trap and Microscope Set-Up

The current lab set-up involves an optical trap used to maneuverer and release the content of gold-coated liposomes (which will be discussed in the next section) and a microscope/camera system used to observe the movements. The high polarizability of the gold nanoparticles enhances the efficiency of the trap, allowing for subcellular light manipulation and making it a desirable mechanism to utilize in the proposed system. However, since liposomes are unstable, they require specific trapping conditions, which will be discussed in this section. The most important aspect of the current laser is that it has a diffraction-limited Gaussian beam, which is required in order to build a good optical trap. The M^2 value is a way to measure the aforementioned quality, with an M^2 value of 1 implying that the beam has the best possible beam quality for a diffraction-limited Gaussian beam. The laser currently used in the optical trap, a Ventus IR (1064 nm, Nd:YAG, CW, 1 Watt) laser, has an M^2 value of 1.2. It also possesses desirable qualities such as a collimated beam with good stability. The laser is pulsed in order to allow for trapping without bursting the liposome prematurely due to constant heat exposure. Although, the lab possesses a beam with a better M^2 value of 1.1, it utilizes femtosecond length pulses, which is too short for the optical trapping process. Our set-up uses 500 ns pulses at 90 mW

for the optical trapping process, which allows for the beam to be on long enough to maintain trap stability. The frequency of these pulses varies with respect to the current usage of the beam, and to how much heat is intended for release into the system. The duty cycle of the beam is another common way to express the amount of time that a beam actively spends on a particle, and corresponds to the amount of heat generated. It is defined as the duration that the laser is active divided by the period of the function, or just the percentage of time that the laser is directed towards the particle. A 10% duty cycle is required in order to maintain stable optical trapping, although the duty cycles currently used in the lab exceed this amount. If the trap is being used to move a gold-coated liposome, then the system uses a 200 KHz frequency (which corresponds to a 20% duty cycle), and if it is being used to release the content of a gold-coated liposome, then the system uses a 1 MHz frequency (which corresponds to a 50% duty cycle). The duty cycle is changed using a Pockels cell, which acts as a shutter to modulate the beam and make it pulse at an extremely high frequency and then alters the duty cycle of those pulses according to operator specifications. The power output of the laser is raised to 250 mW (65 mW average power as the laser is pulsed) and the focus of the optical trap is moved slightly behind the cell to increase the force of the gold-coated liposome and facilitate the insertion of the gold-coated liposomes into cells once they are in the vicinity.

An inverted microscope is used in the set-up, along with an EMCCD camera, which is used because of its increased sensitivity to light, allowing for release patterns to be readily

observed. This allows for the lab members to detect a single liposome and track its movements using the camera. The laser beam is able to be steered by the operator in the x, y, and z directions using a beam steering lens, and allows for the maneuvering of gold-coated liposomes. These changes in position implemented by the operator correspond to very slight shifts on the objective lens, which make very slight changes on the coverslip. This is important because it allows for subcellular shifts in position. A beam expander is used to ensure that the beam fills the objective numerical aperture. The end of the system is comprised of a beam-splitting set-up. This allows for the observation of the optical trapping in the visible wavelength range (because 1064 nm is in the near infrared range) with the addition of a mercury source. Figure 15 shows a diagram of the current set-up while figure 16 shows the actual set-up in the lab.

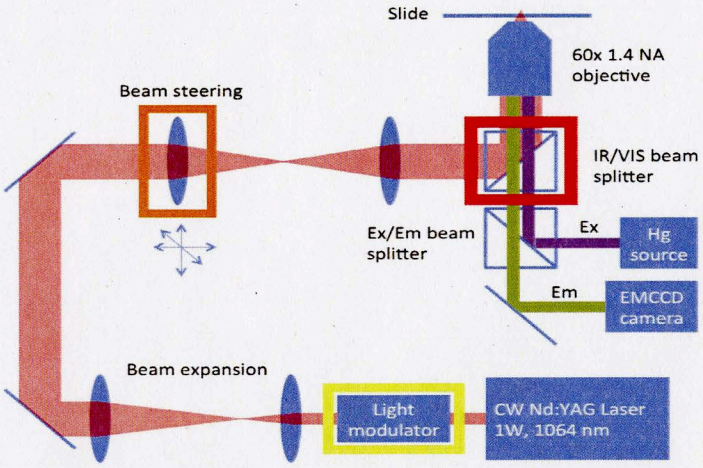

Figure 15. The laser located at the bottom right corner emits a constant wave beam at 1064 nm. It then passes through the Pockels cell light modulator, which pulses the beam and controls the duty cycle of those pulses. The pulsed beam then travels through a set of lenses so that it can expand to fill the objective aperture. Next it encounters a beam steering lens that can be controlled in three dimensions and corresponds to a slight shift of the beam in the sample. Finally, the beam passes through a beam-splitting system so that it can be recorded by an EMCCD camera, and passed through to the sample, which can be viewed using an inverted microscope with a 1.4 NA objective lens (Image from Leung 2011).

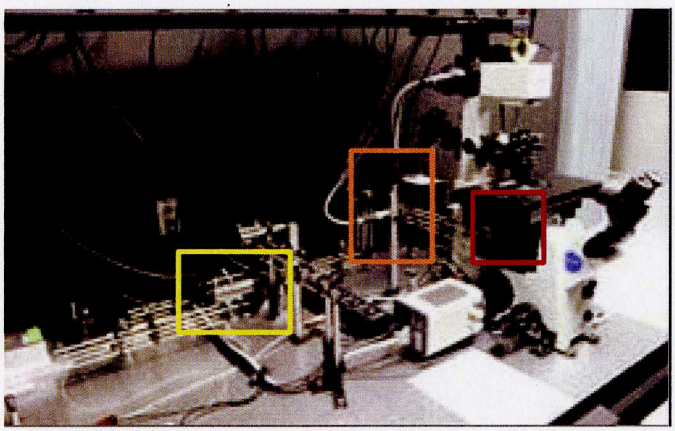

Figure 16. Our current lab set-up. The three boxed items correspond to the boxed items of the same color in figure 14. The item in the yellow box is the Pockels cell. The item in the orange box is the beam steering lens that is controlled by the operator, and the item in the red box is part of the beam-splitting system (Image from Leung 2011).

This system has proven to be very effective for the manipulation of gold-coated liposomes, and even allows for spectral-selectivity as discussed in the next section. Therefore, much of this system is recommended for incorporation into the proposed set-up. Specific equipment that will be required for use will be detailed in the description of the proposed system.

Light-Responsive Liposomes

The utilization of plasmon resonant nanoshells in the lab has allowed for the construction of light-responsive liposomes by coating liposomes with these nanoshells (Troutman 2008). These gold-coated liposomes are advantageous because they can be accurately and precisely maneuvered and opened using an optical trapping system due to the added polarizability from the addition of the gold shell. High plasmon resonance at a specific wavelength allows for the gold shell to optimally absorb light and more efficiently heat the liposome for controlled release in response to a minimum input of light. Thus, they can be loaded with any content and used as a vesicle to deliver content to a specific site where they can be immediately unloaded or released at a controlled rate. Specifically, the lab designs these vesicles for use as drug-delivery systems within the body. The liposomes are prepared using a 90:10:4 molar ratio of the following lipids: DPPC, MPPC to facilitate membrane leakage at the phase transition temperature, and DPPE-PEG2000 to improve colloidal stability (Leung 2011). Gold has become a primary contender for the nanoshell material due to the fact that it is bioinert, and that its refractive index satisfies the plasmon

resonance condition in the visible range, around 530 nm (Troutman 2008). Although gold nanoshells had been used as biomedical markers for imaging purposes, problems arose due to the requirements of complete elimination from the human body (Troutman 2008). For this reason, the lab currently creates the gold nanoshells out of nanoparticles (1 nm), which separate in response to heat generated via infrared laser illumination from the optical trap and become completely eliminated from the body, along with the biodegradable liposomes (100 nm), via renal clearance (which requires particles to be less than 3 nm in size) (Troutman 2008). Even though the shells are formed from nanoparticles, they still produce optical qualities that resemble those of a solid gold shell (Leung et al. 2011). A representation of these gold-coated liposomes and their release tendencies can be seen below in figure 17.

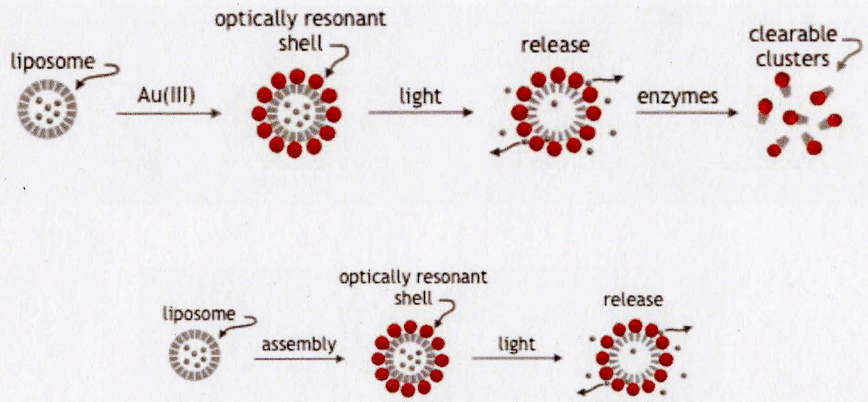

Figure 17. The top image shows the initial liposome (the "soft template"), the liposome with gold nanoparticles added to it, and then the degradation of the initial liposome along with the separated nanoparticles for in vivo purposes. The bottom image depicts a loaded liposome coated in nanoshells that allows for controlled release after an increase in temperature due to the presence of the laser. Note that the liposome is not degraded in this scenario, but simply becoming more permeable. After the laser is no longer illuminating the gold-coated liposome, the liposome will return back to its previous form so it can be optically transported once more (Image from Leung 2011).

Furthermore, these plasmon resonant nanocapsules are spectrally tunable, meaning that various wavelength laser illumination can be used to target the release from gold-coated liposomes with corresponding resonances, while avoiding the release from gold-coated liposomes with non-corresponding resonances. The resonance of these gold-coated liposomes was altered by changing the density of gold nanoparticles on the outer layer of the liposomes, and therefore the mass ratio of gold to lipids. For example, 100 nm liposomes covered in 1 nm gold nanoparticles are resonant within the 760-1210 nm wavelength range. The exact resonance within this range can be achieved by changing the mass ratio mentioned above (473 micrograms of gold per 14.7 milligrams of lipids is resonant at 760 nm and 749 micrograms of gold per 14.7 milligrams of lipids is resonant at 1210 nm) (Leung 2011). It was decided that a pulsed laser beam was the best way to allow for optical trapping while avoiding an increase in temperature that could result in degradation of the particle because it allows for the spatial control of release without heating the surrounding medium (Leung et al. 2011). As discussed previously, a 500 nanosecond pulse is currently used as it eliminates release from off-resonant gold-coated liposomes, allowing for the system to retain spectral-selectivity. Different duty cycles (which represent the time that the pulsing beam is on) are used to switch between trapping and releasing functions and are alternated using a light beam modulator. Currently, a 20% duty cycle is used for trapping as it allows for less heat distribution, while a 50% duty cycle is used for release. A graph depicting the spectral-selectivity of the gold-coated liposomes via light-mediated release can be seen below in figure 18.

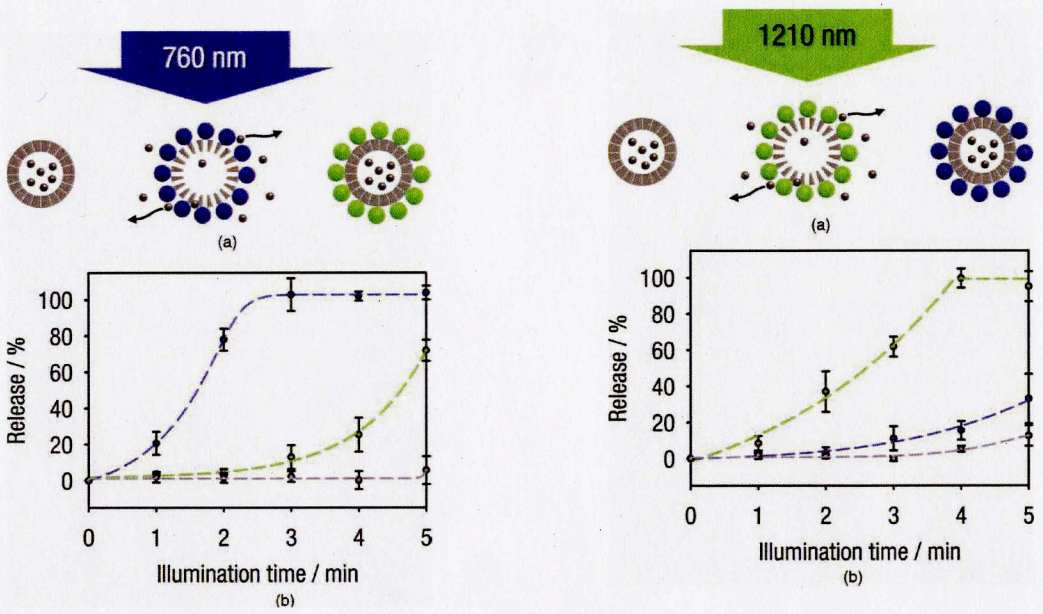

Figure 18. The blue lines in both graphs represent the gold-coated liposomes resonant at 760 nm, while the green lines represent gold-coated liposomes that are resonant at 1210 nm and the grey lines represent uncoated liposomes. It can be seen in the first graph that in the presence of a 760 nm beam, the content release from the 760 nm responsive gold-coated liposomes was at 100% after about 3 minutes, while the content release from the 1210 nm responsive gold-coated liposomes was at roughly 13% and the release from the uncoated liposomes remained at 0%. Likewise, the second graph shows 100% release from the 1210 nm responsive gold-coated liposomes after 4 minutes in the presence of 1210 nm light, while the 760 nm responsive gold-coated liposomes only release about 15% and the uncoated liposomes only release about 5% of their content. This experiment was done using a 0.5 microsecond pulse, with a 10% duty cycle and a 1 W power laser (Image from Leung et al. 2011).

While uncoated liposomes are unstable and are free to move in solution due to Brownian motion, coating them in gold nanoparticles allows for their motion and release rates to be controlled, and for the light-responsive shells to be renally cleared after release. Using a pulsed beam minimizes the effects of heat diffusion to the surrounding media due to the

infrared beam, but a low frequency of 200 KHz still allows for the trap to maintain enough control over the trapped gold-coated liposome. Altering the properties of the gold-coated liposomes allows for the vesicles to exhibit spectrally-selective release. All of these developments made in the lab come together to create a very attractive transport vesicle that can be used not only for in vivo drug delivery, but also for use in the proposed cellular "factory".

5. Proposed Application of Liposomes in Synthetic Biology

As discussed previously, liposomes are commonly used as transport vesicles inside the human body. However, they can also be used as transport vesicles in vitro, as they can be used to help synthesize minimal cells, or a cell-like biomimetic system, by carrying molecules into the synthetic membrane in a more efficient manner than the current methods that were discussed previously. The transport of certain materials into synthetic cells—both for their synthesis and applications—is an important aspect of synthetic biology. Optical trapping along with the utilization of gold nanoparticles is a useful and novel method to facilitate the specific transport of liposomes, and is suggested for use as a method in which liposomes can be transferred into synthetic membranes (GUVs) to deliver components for their synthesis or components necessary for the synthetic cells to carry-out their duties.

The design criteria considered for this process include:

1. The system is able to accurately and precisely load GUVs with the desired content, and is therefore able to obtain reproducible results
2. The system is able to drastically increase the rate of the insertion of components into GUVs (as applied to synthetic cell production and otherwise)
3. The system is able to be easily integrated into the current lab set-up
4. The system is cost effective

The goal is to design a microscopic manipulation system where various molecular compounds are preloaded in liposomes and then carried and released into an empty shell by the means of optical trapping. By performing this operation with a multitude of optical traps and in a microfluidic format, the assembly of synthetic cells can be performed with a high yield evocative of the operation of a factory assembly line. A proposed system that can meet these criteria and goals will be discussed in this section, and contains an optical trapping system, upgraded microscope system, microfluidic chip design, and experimental set-up.

Assembly Line

This optical system described below would be used in conjunction with a custom-designed microfluidic chip to build an efficient "factory-esque" system in which loaded gold-coated light-responsive liposomes could be controlled using the proposed optical trapping system

to deliver content into cellular shells, or synthetic membranes (GUVs). The basic principle of this design is the concept of an assembly line in order to streamline the building process, addressing design criteria 1 and 2. There will be one main channel down which the empty synthetic membranes travel at a constant rate due to surrounding fluid flow. Intersecting this main channel will be a series of smaller parallel channels through which the loaded gold-coated liposomes will travel by independent optical traps. Each of the smaller parallel channels will be supplied with a store of gold-coated liposomes that are all loaded with the same component, and its own optical trap. For example, the first channel could contain gold-coated liposomes loaded with DNA fragment 1, the second could contain gold-coated liposomes loaded with DNA fragment 2, the third channel could contain gold-coated liposomes loaded with ligase, and the fourth, fifth, and sixth channels could each hold a store of gold-coated liposomes filled with a specific marker. The operator could then use this set-up to build three different minimal cells. The first could be filled with content from channels 1 and 4, the second could be filled with content from channels 2 and 5, and the third could be filled with content from channels 1, 2, 3, and 6. Each of these three minimal cells would contain different genomes and different markers, and thus each of them could serve different purposes and be easily identified as type 1, 2 or 3. The operator would be able to see the entire system as they manually direct the correct components into the correct synthetic membranes using the proposed optical trapping system. It is easy to imagine how quickly this process could be carried out, especially if it became automated in the future. For example, a script could be written to instruct the system to rapidly create 50

type 1 cells by turning on only optical traps 1 and 4. Once the optical trapping system is used to transport the correct combination of loaded gold-coated liposomes, it is then used to unload the content from the loaded gold-coated liposomes into the empty GUVs. Once the liposome membranes are repaired (which happens naturally with time, since the heat distributed by the beam is not enough to permanently degrade the liposome), the optical trap can be used again to transfer the empty, unloaded liposomes out of the synthetic membranes and through waste channels where they can be stored for later disposal. A very simplistic diagram of this process can be seen below in figure 19, and a detailed diagram of the microfluidic chip used for the assembly line can be seen in the next section.

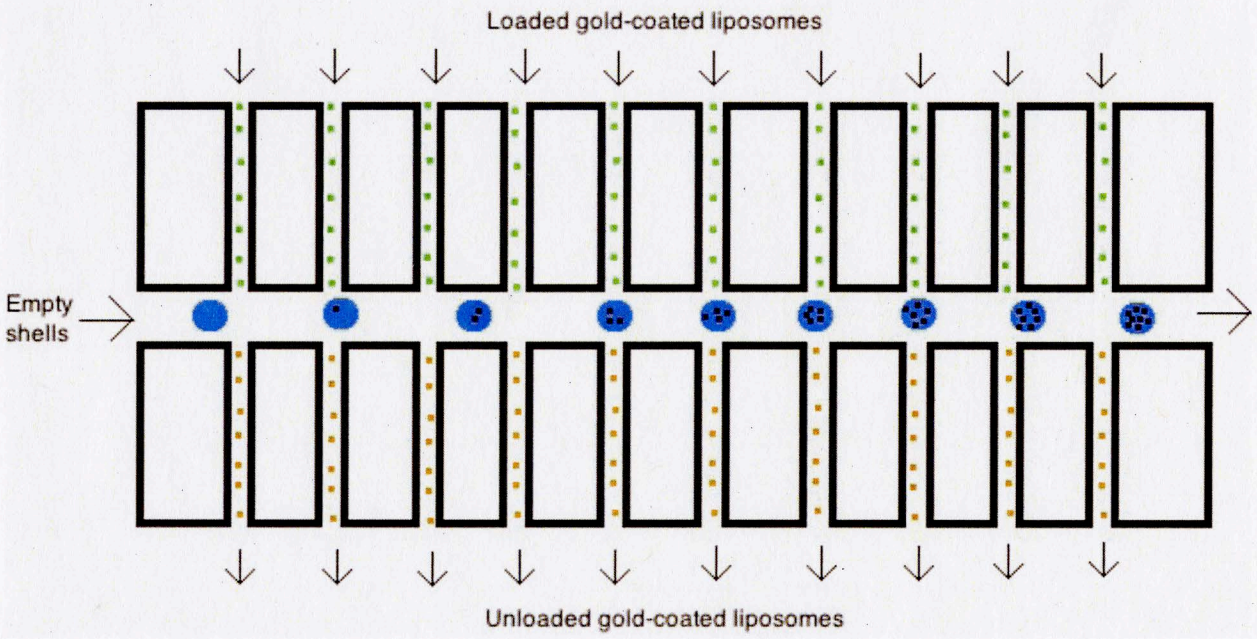

Figure 19. Proposed assembly line system used to assemble synthetic cells using an optical trapping system containing multiple optical traps and gold-coated liposomes as transport vesicles (Image by author).

An optical trapping system capable of controlling multiple optical traps simultaneously already exists and will be discussed later. Currently, the lab is able to manipulate gold-coated liposomes with a singular optical trap, insert them into cells, move them on a subcellular level, and release their content photothermally. These methods can be used to load GUVs with gold-coated liposomes, release their content within the GUVs, and maneuver the empty shells away from the synthetic membrane after unloading. Through the utilization of these methods, the assembly line design could prove to be a very effective method of synthetic cell assembly.

Design of Microfluidic Chip

The assembly line would be most efficiently carried out if combined with a microfluidic chip. The aforementioned channels would be engraved in the chip and thus act as tracts for the optical traps, making the trapping process easier especially if operated manually. There are many important considerations to take into account during the design of this chip to assure that the aforementioned design criteria are met. In order to meet design criterion 3 and allow for easy integration with the current lab equipment, it is proposed that the chip be the size of a microscope slide (3" x 1") so that it will work well with the lab's current inverted microscope. In order to avoid interference with the inverted microscope, it is also important to avoid the placement of tubing or other equipment on the bottom, or even the side of the chip. Although there are many custom microfluidic chip manufacturers, the one chosen for this system was the Microfluidics ChipShop, mainly for their wide range of

products with top entry ports for use with inverted microscopes (Microfluidics ChipShop 2011). Furthermore, the bottom glass layer of the microfluidic chip should be thin enough to maintain the efficacy of the beam so that the trapping and release mechanisms will be accurate; the minimum thickness able to be manufactured was found to be 150 microns, which is ideal for the proposed system. The top layer of the chip (above the channels) is always constant at 2 mm, according to the manufacturers considered. The channel size is also important to ensure proper flow through the chip. Too small of a size (near 10 microns in diameter) can result in high shear stress and inconsistent boundary layers which would impede the process and discourage reproducible results, while too large of a size can result in unorganized flow of particles and rough, turbulent flow, particularly through the main channel where movement depends entirely on the fluid flow and the synthetic membrane flow must be single-filed and constant. It is proposed that the center channel is 100 microns in diameter (assuming the use of synthetic membranes with a 50 micron diameter), and that the parallel delivery channels are 20 microns in diameter (assuming the use of gold-coated liposomes with 100 nm diameters). This was decided partially based on the fact that the chosen custom chip designer employs these diameters as standard channel sizes (Microfluidics ChipShop 2011). However, custom microfluidic chips can also be made to order from a variety of companies, if all these dimensions are specified. A diagram containing the dimensions of the proposed microfluidic chip can be seen below in figure 20.

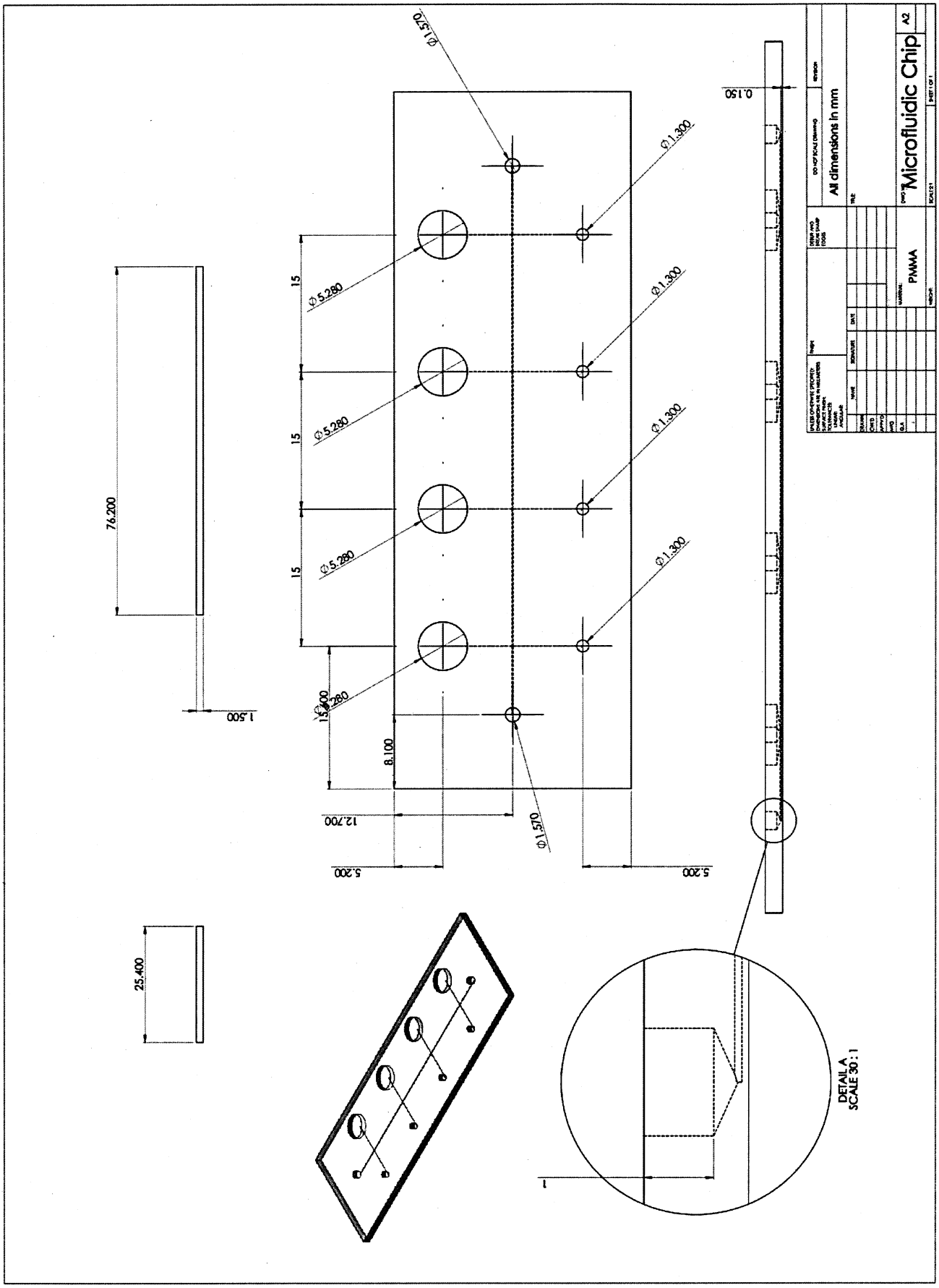
Microfluidic Chip
All dimensions in mm
PMMA
A2
DETAIL A
SCALE 30 : 1
76.200
1.500
25.400
0.150
1.570
1.300
5.280
15
8.100
12.700
5.200

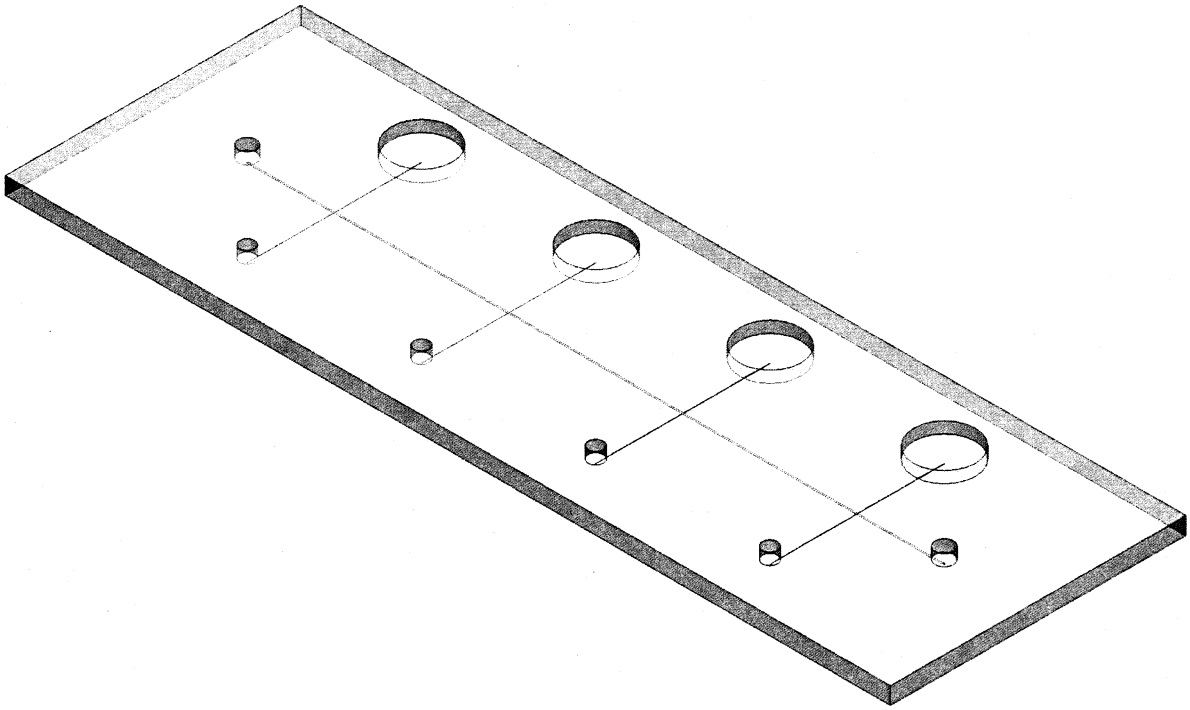

Figure 20. The top image is a diagram containing the dimensions of the custom microfluidic chip from multiple perspectives. The bottom image is an isometric view of the custom microfluidic chip. The back four entry ports are where the storage tanks will be inserted, the front four are where the female luer locks will be placed, and the end two ports are sized for the Upchurch nanoports (Image designed in SolidWorks by the author).

After choosing Microfluidics ChipShop as the most applicable manufacturer due to their line of products that access the custom chips from the top, their materials and accessories were evaluated for use with the proposed system's design criteria. For this particular type of microfluidic chip design, materials that offered include the transparent polymers PMMA

and Topas. Since water will be the fluid in which the synthetic membranes and gold-coated liposomes travel, it is important that the material used is hydrophilic, or that a hydrophilic coating is applied to the interior of the channels. It is also important to consider whether or not the material allows for light emission in the proposed spectral range (both 400-600 nm and 760-1210 nm). PMMA is a widely used material known as plexiglas and is inexpensive but prone to scratching. It does not filter out light in the proposed spectral range, however it is hydrophobic, so that it can be used but would require a hydrophilic coating (http://en.wikipedia.org/wiki/Poly(methyl_methacrylate)). Topas is quite similar, in that it also does not filter out light above 300 nm, and that it is also hydrophobic (http://www.topas.com/topas_brochure_english.pdf). The prices of a microfluidic chip in each material are equal (the manufacturer specifies a price of between $31.00 and $57.00 depending on the number of chips bought), and both would require a hydrophilic coating, so the material used is irrelevant (Microfluidics ChipShop 2011). However, it should be noted that while the price of an off-the-shelf microfluidic chip with comparable channel sizes is low, the price of a custom microfluidic chip might be significantly higher. This is because the chips are most likely mass produced using a mold, and a custom chip would require a custom mold, which could cost tens of thousands of dollars. Therefore, it is recommended that the Microfluidics ChipShop be consulted before ordering a custom chip, as they may have a comparable design for sale at a much lower price.

There are a wide number of accessories that can be used to store the gold-coated liposomes and to distribute water and synthetic membranes to the system. In order to adhere to design criteria 1, 2, and 4, accessories were evaluated based on their storage capacities, ease of use, integration with the assembly line system, and cost. The four accessories proposed for use are the Upchurch nanoports, the capillary PEEK tubing, the female luer lok connectors, and the tanks offered by Microfluidics ChipShop. For interfacing purposes, the manufacturer provides male mini luer fluid connectors, female luer lok compatible connectors, and Upchurch nanoports (Microfluidics ChipShop 2011). While all three allow for connections with many devices such as tubing and syringes, the Upchurch nanoports were chosen for use as connectors to the pump system at the ends of the primary channel due to their low cost at around $21 for 20 Upchurch nanoports (Microfluidics ChipShop 2011). They also allow for connection to the capillary PEEK tubing, which is the only tubing sold by the Microfluidics ChipShop, and will be used for the transfer of fluid through the system ($80 for 10 pieces of tubing) (Microfluidics ChipShop 2011). The tubing used in the system will have an outer diameter of 1/32" and each piece has a length of 12" (Microfluidics ChipShop 2011). It will go from the end of the main channel to a reservoir where finished synthetic minimal cells will eventually be drawn from. More tubing will be used to introduce fresh water and empty synthetic membranes into the system and will be attached to a pump to maintain a constant laminar flow. The nanoports have a footprint of 8.4 mm, and require a 1.57 mm diameter entry port, which can be seen in the design of the chip in figure 20. Below, in figure 21, an image of an Upchurch nanoport can be seen.

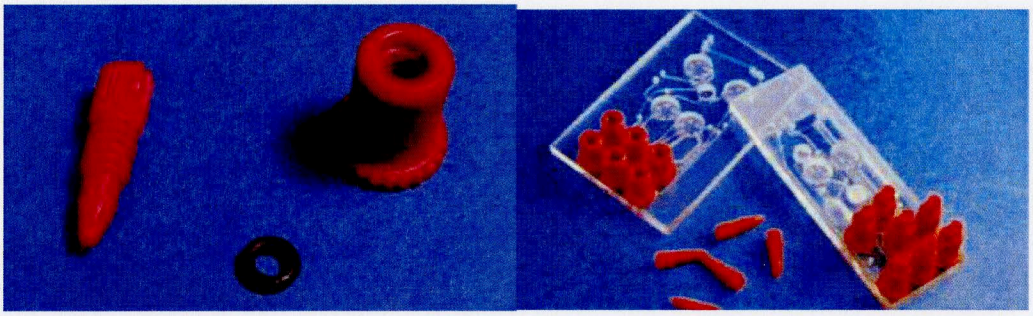

Figure 21. On the left is an Upchurch nanoport assembly set, and on the right is a sample microfluidic chip with the Upchurch nanoports inserted (Image from Microfluidics ChipShop 2011).

For the storage of loaded gold-coated liposomes, it was important to only consider methods that store solution directly on the chip. This will help to achieve the 2nd design criterion by assuring a fast transfer of solution to the microfluidic chip channels. The Microfluidics ChipShop offers two types of storage accessories that can be mounted on the chip: tanks and blister pouches. Due to the easier reloading capabilities of tanks, they were chosen for loaded gold-coated liposome storage. Tanks will be used to store loaded gold-coated liposomes at the entrance site of each of the parallel channels. These are small capsules that hold up to either 500 microliters or 4.5 milliliters and can release their content using either a mechanical piston or pneumatic pressure (Microfluidics ChipShop 2011). The 500 microliter tanks were chosen because they are less expensive, at $7 for 10 tanks (if ordered in batches of 100 tanks), and because the volume of storage required for the system is minimal (Microfluidics ChipShop 2011). The 500 microliter tanks are able to be plugged directly into the chip (Microfluidics ChipShop 2011). An image of these tanks, along with

their dimensions can be seen below in figure 22. It can be seen that the footprint of the tank is about 7.5 mm, and that the base that is plugged into the chip is 5.28 mm in diameter, which corresponds to the holes above the channel ends in figure 20.

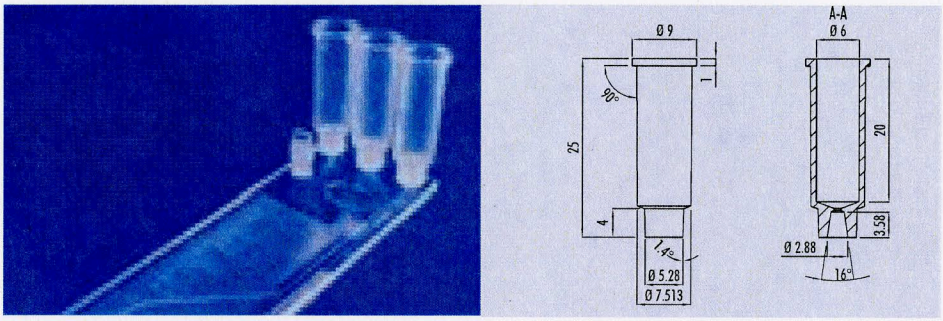

Figure 22. On the left, three tanks are shown inserted into a sample microfluidic chip. On the right are the dimensions of the tank (Image from Microfluidics ChipShop 2011).

Lastly, it is important to consider what happens to the waste liposome parts after they are removed from the main channel and have traveled down the exit channels. While a second pump system could be used to continuously remove waste, it is not recommended because it will interfere with the perpendicular flow in the main channel. Furthermore, as both a pump and tubing are rather expensive, it would be more cost effective to remove the waste via other means. It is proposed that since the exit channels are small, waste will remain at the end of the channels after being moved there by the optical trapping system, and that it will not diffuse back to the main channel (due to the perpendicular flow) or spontaneously be taken back into the loaded synthetic membranes. It is proposed that the entry ports above the waste stream ends are made to fit female luer loks, so that they can easily

interface with syringes (which have male luer connection fittings). Additionally, syringes can be purchased with built-in female luer loks, so that they can be directly inserted into the microfluidic chip for waste syringing. The female luer loks require a 1.3 mm entry port in the chip, which can be seen in figure 20. The cost for female luer loks is about $15 for 10, if they are ordered in batches of at least 20 (Microfluidics ChipShop 2011). The waste should be maintained at the end of the exit channels until the microfluidic chip is done synthesizing cells. Then, the operator can syringe the waste out of the exit channel ends without interfering with the system as the process is underway.

The Dolomite Mitos P-pump was used for throughput calculations (which will be discussed later), and is an ideal pneumatic pump for this system due to its pulseless flow in the nanoliter/min to microliter/min range, which is required for this process (http://www.dolomite-microfluidics.com/webshop/pressure-pumps-modules-c-38_41_42/mitospump-p-724). However, a quote for this piece of equipment was not obtained. The total cost of this proposed microfluidic chip system (not including the pump and the syringes, which are already readily stocked in the lab) is around $1,027 and can be seen detailed below, in table 1.

Costs Table 1

Item	Bulk Number	Bulk Price	Number for 1 Complete Device	Price for 1 Complete Device
Microfluidic chip	1	About $1,000 ($57 for duplicates)	1	$1,000
Upchurch nanoports	20	$21	2	$2
PEEK capillary tubing	10 12" pieces	$80	2	$16
Storage tanks	10	$7	4	$3
Female luer lok connectors	10	$15	4	$6
TOTAL				**$1,027**

Table 1. The required components to build the proposed microfluidic chip (All prices from Microfluidics ChipShop 2011).

Proposed Multiplexed Optical Trap System

It is believed that the current optical trapping system utilized by the lab could be improved upon to allow for the independent controlled movement of multiple gold-coated liposomes through the microfluidic chip. Recent developments in optical trapping technology has led to the creation of a single-beam gradient force optical traps with higher trapping precision and improved calibration of forces and displacements, such as the trap utilized by the lab (Neuman 2004). With the use of this optical trap in conjunction with a polarizing beam splitter or a spatial light modulator (SLM), multiple optical traps can be generated and manipulated simultaneously in one system.

While most optical trapping systems are able to maneuver molecular components using one independently controlled beam at a time, the incorporation of polarizing beam splitters or spatial light modulators have allowed for the independent control of two or more particles using one multiplexed beam. Polarizing beam splitters split a beam into two beams of different polarization that can then be controlled independently, however spatial light modulators can drastically increase the number of independent beams (http://en.wikipedia.org/wiki/Polarizer). Spatial light modulators are based on a translucent or reflective liquid crystal microdisplay and spatially modulate light by both amplitude and phase (http://www.holoeye.com/spatial_light_modulators-technology.html). Each pixel on the microdisplay can individually control the phase or amplitude of light either passing through it or reflecting off of it, meaning that each pixel is essentially corresponding to its own optical trap—allowing for up to 200 independent optical traps per SLM system (Savage 2009). The operator controls the multiplexed optical trap by altering the pattern of light distribution among the pixels. The most prominent manufacturers of spatial light modulators include Holoeye and Hamamatsu, and Holoeye was chosen for the proposed system due to the fact that a Holoeye SLM was used in the multiplexed optical trapping system set-up that is referenced below (in figure 25). The addition of a spatial light modulator to the current optical trap specifically addresses two of the design criteria. It will make the system more rapid, and it is easily integrated into the current system. However, while spatial light modulators are still extremely important to the success of the proposed process, current SLMs can only define a new pattern at a rate of

180 Hz, meaning that an SLM system could not be used to pulse the current laser beam (which requires pulsing up to 1 MHz), and would have to be used in conjunction with a Pockels cell.

The proposed multiplexed optical trapping system was developed in reference to one created by Richard Bowman and Miles Padgett of the Department of Physics and Astronomy at the University of Glasgow in May 2010 (Bowman, Preece, Gibson, and Padgett 2011). Their system consists of a stereoscopic particle tracking system with a spatial light modulator and a user-friendly interface so that the operator can control multiple particles in three dimensions. Together, these systems allow for the collection of quantitative position data and qualitative depth perception (Bowman, Preece, Gibson, and Padgett 2011). The system has been developed to attain maximum three-dimensional tracking accuracy by use of a software interface. Users were originally able to control the individual particles by use of a three-dimensional haptic interface using a gaming joystick while the forces on the particle were measured in real-time (Bowman, Preece, Gibson, and Padgett 2011). However, in November 2010, the same research group expanded on this work to develop a more accessible user interface system called the "iTweezers" (Bowman, Gibson, Carberry, Picco, Miles, and Padgett 2011).

The iTweezer system is again a three dimensional haptic interface, and allows for the manipulation of multiple particles with holographic optical tweezers using an Apple iPad serving as a remote monitor and control device (Bowman, Gibson, Carberry, Picco, Miles, and Padgett 2011). It consists of a downloadable application through the Apple Store, and corresponding LabVIEW software that allows for easy manipulation of up to 11 optical traps due to the use of a computer-controlled spatial light modulator to multiplex and alter the intensity of a laser beam (Bowman, Gibson, Carberry, Picco, Miles, and Padgett 2011).

The iPad was chosen by the Bowman and Padgett group for its ten-inch color screen with capacitive touch sensor, and its Apple gesture recognition toolkit, which allows the fingers to be tracked at 200 Hz and accounts for the continuity and smoothness of the system (Bowman, Gibson, Carberry, Picco, Miles, and Padgett 2011). The user is able to interact with the microscope image and the overlaid optical trap markers displayed on the iPad, as seen below in figure 23. The iPad's accelerometer is also utilized so that the microscope stage can be translated by tilting the iPad (Bowman, Gibson, Carberry, Picco, Miles, and Padgett 2011). Then, the coordinates determined by the user's hand motions are synchronized with a desktop computer using LabVIEW software, which then controls the spatial light modulator (Bowman, Gibson, Carberry, Picco, Miles, and Padgett 2011). This system allows for relatively inexperienced users to easily and precisely trap particles, move them, and translate the microscope stage.

Figure 23. Here the iTweezers interface can be seen in action. Guiding a particle with a fingertip moves it in the xy-plane, while using a pinching gesture to stretch or squeeze a marker with two fingers moves the particle in z-space. There is an online video that demonstrates the same principle at stacks.iop.org/JOpt/13/044002/mmedia (Image from Bowman, Gibson, Carberry, Picco, Miles, and Padgett 2011).

Although the iTweezers system is not unique in its ability to utilize a spatial light modulator to manipulate multiple optical traps (http://ptonline.aip.org/journals /doc/PHTOAD-ft/vol_62/iss_2/26_1.shtml?bypassSSO=1), it is the focus of this report due to its availability, cost, and ease of use. The iTweezers software as an interface for the multiplexed optical trap will address all four of the design criteria. It will allow for precise and accurate manipulation of the independent beams, it will allow for fast movements and therefore a higher throughput, it is easily integrated into the current system, and it is available at no cost. It is proposed that this optical trapping system be used for the improved manipulation of liposomes, which can result in the more efficient and accurate assembly of synthetic cells as relevant to the field of synthetic biology.

The iTweezers system is currently available at the iTunes Application Store for free, and also requires the PC software created by Bowman et al., which is entitled "Red Tweezers" and consists of a LabView 8.6 library, a stand-alone OpenGL hologram engine, and a windowed version of the hologram engine (http://itunes.apple.com/us/app/itweezers/id456952257?mt=8). This software can be downloaded for free from this website: http://www.physics.gla.ac.uk/Optics/projects/tweezers/software/. This technology could be combined with the current lab set-up in order to make the proposed assembly line system a reality.

Proposed Optical Trap and Microscope Design

The set-up of Bowman and Padgett's team will be discussed in this section, and the differences between this system and the current system in the lab will be mentioned. Bowman and his team have used a simple approach to tracking each particle in three-dimensions, which is the utilization of a high-speed camera (Prosilica GC640M) instead of a quadrant photodiode, which is typically used (Bowman 2010). This allows for a simple calibration and allows for multiple particles to be tracked at the same time (Bowman 2010). Luckily, a high-speed camera is currently used in the lab, as mentioned previously, and will help with the realization of the multiplexed optical trap set-up. Stereomicroscopy, or a modified microscope, is used along with the high speed camera to achieve this, however, a commercial stereomicroscope is not recommended due to its need for a large

optical system and special sample cells (Bowman 2010). The mechanism in which stereo images are produced can be seen below in figure 24.

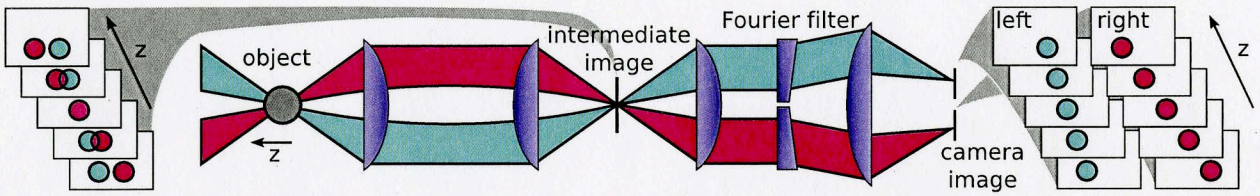

Figure 24. Illustration of how the imaging system produces stereo images. An intermediate image is created with a two-lobed point spread function and then is re-imaged using a Fourier filter where it is split into two views from different angles. The only image analysis that is required in stereoscopic imaging is the tracking of objects in 2D (Image from Bowman 2010).

Instead of a commercial stereomicroscope, an inverted microscope arrangement with a high numerical aperture (N.A.) objective lens (Zeiss Plan Neofluar, oil immersion, x100, N.A. 1.3) was used by Bowman's team to image the sample onto an aperture and then re-image it onto the high speed camera using a Fourier domain filter to separate the image into a stereo pair (figure 24) (Bowman 2010). The optical tweezers system is coupled in after the first aperture with a dichroic mirror, and then an expanded laser beam illuminates the SLM (Holoeye LC-R 720), which is re-imaged onto the back aperture of the objective (Bowman 2010). Two lengths of acrylic light-pipe fibers with 1.5 millimeter diameters are placed about 1.5 millimeters above the sample without a condenser lens and illuminated by white LEDs, which produces an image at the focal point of the tube lens with a two-lobed point spread function (figures 24 and 25B) (Bowman 2010). The separation of these two

images from the point spread function are separated by a distance that is linearly proportional to the depth of the sample (Bowman 2010). This phenomenon can be seen below in figure 25B, while an image of Bowman's specific set-up containing all the aforementioned components can be seen in image 25A.

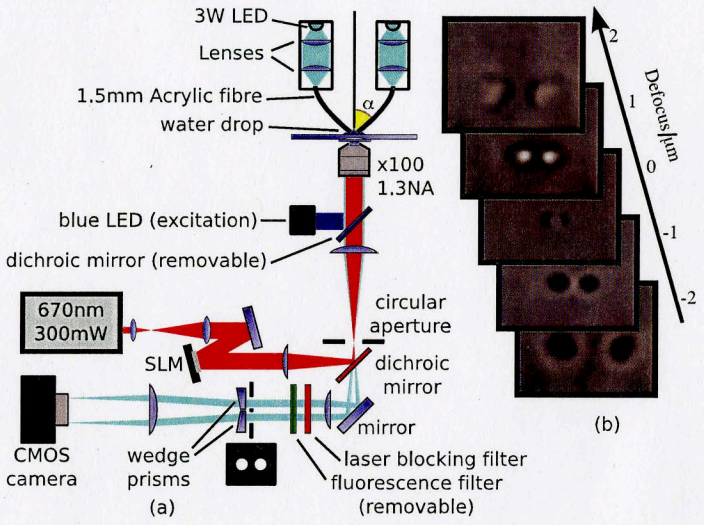

Figure 25. The optical system used for Bowman's stereoscopic imaging in optical tweezers can be seen in image A, and the images of a 2 micron bead at different depths, although without the prisms to separate the images (Image from Bowman 2010).

When comparing this system to the current lab set-up, it is immediately noticed that the two are quite similar. Both utilize a high-speed camera, a high N.A. objective lens, and an inverted microscope, which are all standard for optical trapping systems. The differences mainly reside within the laser and the presence of a spatial light modulator. The laser used by Bowman et al. is a continuous wave laser, similar to the one utilized in the lab. However, it operates at 670 nm and 300 mW. While this does not imply that the current laser would

need to be replaced with one of this nature, it does mean that a different SLM would need to be used with the current laser. The SLM used by Bowman and Padgett works well for their 670 nm CW laser, but would not diffract light efficiently at 1064 nm. Unfortunately, a spatial light modulator that diffracts light efficiently at 1064 nm is about three times the cost of one that works at 670 nm.

Due to this high cost, the biggest addition to the current system would be the spatial light modulator that is required to establish multiple independent optical traps. Unlike the Romanowski lab set-up, Bowman's set-up does not include a Pockels cell to pulse the beam and change the duty cycle, as they are not concerned with heat diffusion to the surrounding media, and instead use a continuous beam. As mentioned previously, a maximum refresh rate of 180 Hz is certainly fast enough to get clear movement of the trapped particles using the iTweezers application, but it is not fast enough to eliminate the need for a Pockels cell, since a Pockels cell is able to modulate light at least at our required 1MHz rate (http://www.holoeye.com/download_daten/Spatial_Light_Modulator_LC-R_720.pdf). This is important because it requires modulation by a Pockels cell before the beam enters the SLM, meaning that all of the independent optical trap will need to be at either 200 kHz or 1 MHz. It will not be possible to trap a particle with one independent trap and release content from a particle using another independent trap simultaneously. In order to maintain the frequencies employed by the lab today, and eliminate the need for a Pockels cell, the frame rate needs to increase by almost 6000 times.

If SLM technology is not able to improve by that magnitude, but is able to be increased by 1000 times to allow for trapping pulse frequencies, then perhaps a secondary continuous wave laser that is stationary at the end of the main channel could be used for releasing purposes. When the loaded synthetic membranes reach the end, the beam will cause photothermal release of liposomal content and the operator can then remove the remaining liposome pieces out into an exit channel. This would allow for the SLM to operate at a lower frame rate, since it will only be used for trapping and not for inducing release, and would allow for the Pockels cell to be eliminated from the system.

The pertinent components of the proposed optical trap and microscope set-up are listed below in table 2. These could be utilized along with the current lab set-up in order to replicate the system utilized by Bowman et al. in the development of the iTweezers. Every component of the proposed system is included in the table, including items already owned by the lab such as the high-speed camera and high N.A. objective lens. The application can be downloaded for free from the iTunes Application Store, and the software can be downloaded for free from the aforementioned website. After all of this is done, the system could be used to transport liposomes into and within cells with the use of the proposed microfluidic chip. The overall cost of this optical system is about $100,244 (or $18,499 in additions to the current Romanowski lab equipment), as indicated below:

Costs Table 2

Item	Manufacturer	Details	Price
Spatial light modulator[1]	Holoeye	SLM Pluto NIR	$18,000
High speed camera*[2]	Hamamatsu	Electron multiplier CCD camera	$31,750
Microscope including High N.A. objective lens*[3]	Olympus	Inverted, Oil immersion, N.A. of 1.42	$30,783
Laser*[4]	Laser Quantum	Ventus CW 1064nm 1W Laser	$8,750
Pockels Cell*[5]	Conoptics Inc.	For 1064 nm laser, 30 MHz frequency,8 ns rise/fall time, 175 V max.	$10,463
Apple iPad[6]	Apple		$499
iTweezer iPad Application[7]	Bowman Lab	iPad-based software	Free
Red Tweezers[8]	Bowman Lab	LabView-based software	Free
TOTAL			**$100,244**

* indicates already owned

[1]Quotation, Holoeye, 2011
[2]Quotation, Hamamatsu, 2011
[3]Quotation, Leeds Precision Instruments, 2011
[4]Quotation, Laser Quantum, 2010
[5]Quotation, Conoptics Inc, 2011
[6]http://www.apple.com/ipad/
[7]http://itunes.apple.com/us/app/itweezers/id456952257?mt=8
[8]http://www.physics.gla.ac.uk/Optics/projects/tweezers/software/

Table 2. Primary components required to build the proposed optical trapping system.

Design of the Empty Shell

Giant vesicles (GUVs) can be utilized as the synthetic cell membranes—or, as the empty shells that will be loaded with gold-coated liposomes. The material inside the smaller, gold-coated liposomes will be inserted and permanently encapsulated inside the GUVs, while their liposome casings will be removed and discarded. When considering the best method available to produce these GUVs, it is important to again remember the four design criteria. The GUV synthesis process applies to the 1st, 2nd, and 3rd. It should result in consistently sized GUVs so that the results of each experiment using the proposed design are reproducible. Also, the formation method should be fast, and it should be cost effective. The most appealing synthesis method is one that meets all of these criteria. It was developed by Stachowiak et al. at the University of California-Berkeley and involves the use of microfluidic jet pulses to form GUV "bubbles" from unilamellar membranes (Stachowiak 2008). A pulsatile jet is directed onto a unilamellar lipid bilayer that is formed between two aqueous phases, and releases a micropulse of fluid, which deforms the bilayer, creating the GUV as shown in figure 26 (Stachowiak 2008). The method was used to generate GUVs around 200 microns in size, which is applicable for the proposed system, at a fairly consistent rate (Stachowiak 2008). It is also low cost, because the same lipid bilayer can be used to generate many GUVs since the bilayer remains intact after each GUV is formed (Stachowiak 2008). Finally, the method results in the creation of GUVs in rapid succession, as the formation time per GUV is only 5 ms (Stachowiak 2008). This system could even be

integrated into the assembly line so that GUVs are created on demand and released into a reservoir before they are pumped to the microfluidic chip.

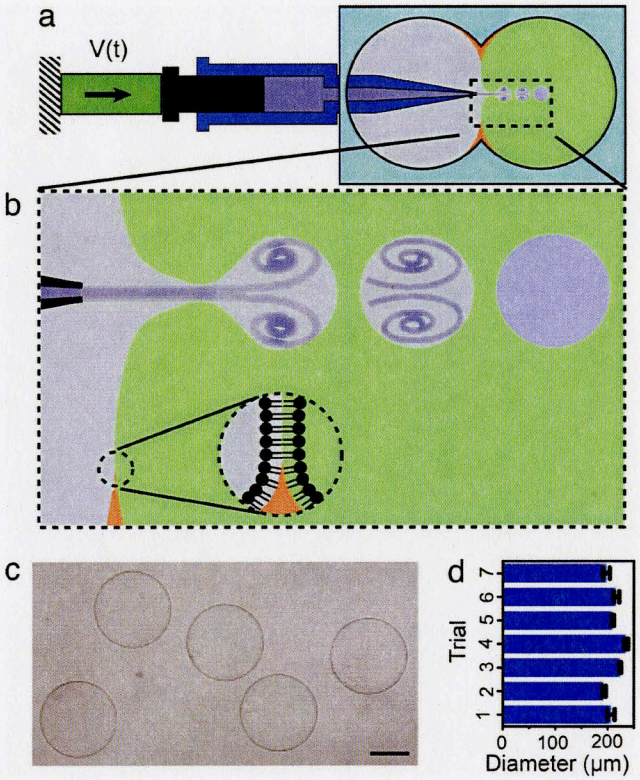

Figure 26. Image A shows the microfluidic jetting device with the lipid bilayer chamber. Image B is a close up of the vesicle formation process. Image C shows independent, monodispersed GUVs, and image D shows the consistency of vesicle diameter over 7 trials resulting in 46 GUVs (Image from Stachowiak 2008).

Although the previous method meets all of the aforementioned criteria, it does not result in GUVs that closely resemble natural cell membranes because it must be done in low ionic conditions. Another possible method that avoids this problem was first utilized by Estes and Mayer in 2005, and allowed for them to form the vesicles using a process called

electroformation. This allowed for the vesicles to be the size of living cells, or about 10-100 microns, to better model the synthesis of synthetic cells. Essentially, an AC current induces an electric field, which instigates the formation of GUVs from a film of lipids that are on one or both of the electrodes, and are separated by an aqueous solution (Estes 2005). Low ionic strengths are stereotypically required for the electroformation process to be successful, because ions enter the space between the lipid bilayers on the electrode surfaces and impede bilayer separation, and therefore the formation of GUVs (Estes 2005). A low ionic strength, however, does not accurately model a living cell, making this synthesis technique less than desirable, and leading to the common use of PEGylated lipids for liposome production. The authors of this article managed to build a GUV at high ionic conditions without the use of chemically-modified lipids that are usually employed in the formation of lipid vesicles (Estes 2005). First, a flow chamber set-up was used to employ the electroformation process at low ionic conditions to create the GUVs (Estes 2005). In order to avoid the problem of reduced lipid bilayer separation caused by the low ionic state, which discourages the formation of GUVs, high ionic strength solutions were then added after forming the GUVs, so that they better represented living cells (Estes 2005).

The GUVs produced using this method have one drawback; they are attached to the surface on which they were created. This creates a problem because surface-attached liposomes do not permanently entrap ions or small polar molecules, and would be difficult to employ in the set-up described in this report (Estes 2005). This would not meet the design

criterion of a fast process, because the GUVs would have to be somehow removed from the surface after production. However, the authors were successful in trapping larger molecules (such as enzymes) inside the GUVs for about 24 hours without significant losses (Estes 2005), which is promising. Experimental attempts can be made to remove the produced GUVs from their surfaces, so that they can flow down the main channel of the proposed microfluidic chip, although the first method is still recommended unless the GUVs must resemble natural cells.

If the GUVs must resemble natural cells and the GUVs created via Estes's method cannot be removed from their surfaces experimentally, then there are many other methods that can be used. For example, Schwille's lab utilizes electroswelling, a process in which GUVs are grown from a pellet of natural membrane pieces (Merkle 2008). Furthermore, in the future it may be of interest to design GUVs with a more flattened shape, so that they more closely resemble natural cells. However, for the purpose of this system, that is not a requirement (Mouritsen 2011).

Nanoparticle Markers

The presence of a labeling system is crucial to the design process. As mentioned during the description of the assembly line, gold-coated liposomes loaded with markers could be added to specific synthetic membranes in order to signify the contents of the completed

synthetic or semi-synthetic cell, so that each type has a sort of serial number. Todays scientists use three common forms of markers—lanthanide bars, fluorescence dyes, and quantum dots (White 2009, Fortina 2005). Because the gold-coated liposomes are so small, these markers would have to be on the nanometer scale. Lanthanide bar markers are attractive because they are used to create markers that entail a series of colored stripes on a bar, similar to those on a resistor. Using this method, one could create a specific bar code about each type of synthetic cell that allows an observer to gain information about the cell just be viewing a series of lines. However, because of the nanometer scale requirement, they are out of the question, since these bars would likely be the same size as the GUVs. Fluorescent dyes are not possible because they cannot be controlled via an optical trap. Quantum dots—or fluorescent molecule markers—are the most attractive of these options due to their size. They are nanometer-sized crystals that are excitable by UV and visible light, and emit a color corresponding to their size (http://www.viewsfromscience.com/documents/webpages/nanocrystals.html). However, since each particle only emits one color, multiple quantum dots would have to be added to each synthetic membrane in order to create more label options for the vast amount of possible cell types. This is because it is important for the labels to be easily differentiable with the use of spectroscopy, so having one that emits a blue light, and one that emits a blue-green light would not be useful system. Additionally, there is another method that is not commonly used, but that can be utilized for this system in an extremely similar manner as quantum dots would be used. Currently, the lab is developing up-converting

nanoparticles, which are nanocrystals doped with lanthanides. The doped nanocrystals can then emit red, green, or blue light, or a ratio of all three. It could be possible to vary these ratios with enough spectral significance so that a wide number of markers could be created. Because each nanocrystal is doped with varying ratios of lanthanides, only one nanocrystal would need to be loaded into each synthetic membrane, as opposed to the multiple quantum dots that would need to be loaded into each membrane to produce spectrally significant ratios of varying light wavelengths.

Example of Loaded Liposomes

These loaded, gold-coated liposomes could be loaded with a very wide variety of biological materials in order to accomplish many possible tasks, which will be discussed in the next section. One example is the loading of smaller strands of DNA or RNA along with ligase enzymes so that they can be assembled into longer strands of genome that are too long to fit into a liposome delivery vesicle. Loading liposomes with genome parts could be used to replace current transfection methods, and make them more efficient. Additionally, there is a Registry of Standard Biological Parts at MIT, which is a collection of biological parts that can be bought individually and mixed-and-matched to assemble synthetic cells containing the parts of your choosing (http://partsregistry.org/Main_Page). Parts found on this website are perfectly suited to be used for this application. Examples of parts available at the Registry of Standard Biological Parts are promoters, protein coding sequences, terminators, DNA, plasmids, and primers. The website is extremely easy to navigate and

users can create an account to order the parts needed to build their ideal synthetic cell. Finally, ideas of parts combinations can be found at the International Genetically Engineered Machine (iGEM) Foundation website (http://igem.org/). iGEM is a competition in which undergraduate students receive a "kit" of biological parts from the Registry of Standard Biological Parts and attempt to design and build their own biological systems. Example products developed by students during this competition can be seen on the iGEM website. Below, in figure 27, is an example of a kit of biological pieces that are purchased from the Registry of Standard Biological Parts and used to assemble a synthetic cell.

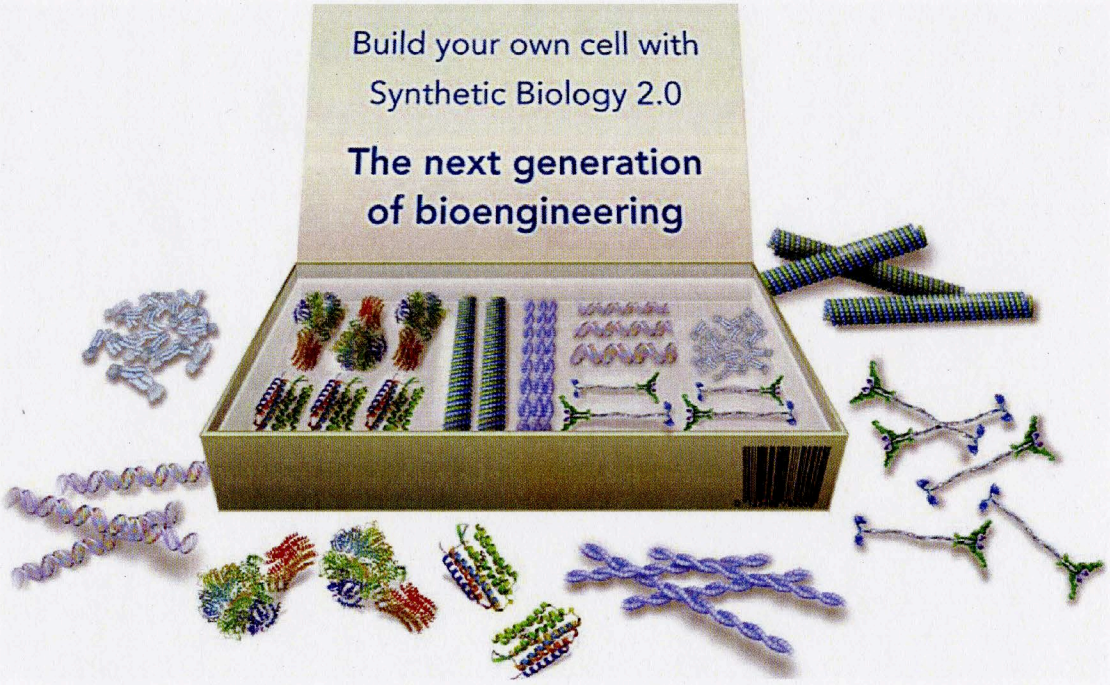

Figure 27. An illustration of a hypothetical kit of biological parts obtained from the Registry of Standard Biological Parts (Image from Schwille 2011).

Proposed Experiments

Once this system can be developed, its usefulness can be demonstrated by performing a simple experiment with the system. One such experiment would be the release of substrates and their enzymes into a GUV nanoreactor to observe their fluorescent products. An experiment containing this process was done by Bolinger et al. in 2008, so the results would be able to be compared to a previous experiment to assure the success of the new system (Bolinger 2008). Two types of liposomes were loaded into a GUV (one type loaded with DDAO phosphate, and one type loaded with FDP) in the presence of alkaline phosphatase, and released by thermal release mechanisms. First, the temperature was increased to 23 °C, which released the DDAO phosphate, and resulted in the conversion of DDAO phosphate to DDAO, releasing a light red fluorescence emission (Bolinger 2008). Then, the temperature was increased to 41 °C to release the FDP, which was then converted to fluorescein, releasing a light green fluorescence emission (Bolinger 2008). The completion of this experiment would allow for the testing of the efficacy and reproducibility allowed by the proposed system. An illustration of the proposed experiment can be seen below in figure 28.

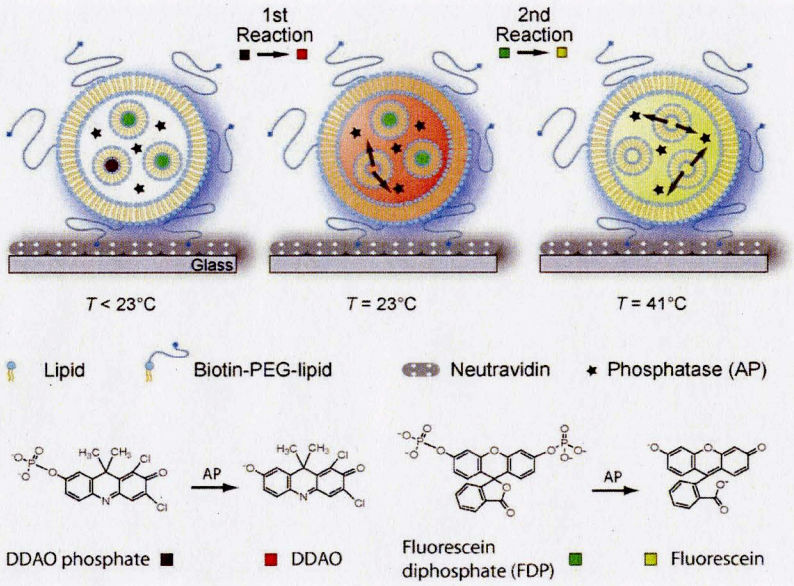

Figure 28. A diagram of the aforementioned process where the stars represent the enzyme alkaline phosphatase and the other colors are described by the key at the bottom of the image (Image from Bolinger 2008).

A second proposed system is one that can be used to calculate the throughput of the system based on a proposed pump and to model the GUVs as batch reactors. These calculations are assuming that it is necessary for the components in the GUVs to react completely before any other components are added, so that it is crucial for the residence time inside the reactor to be shorter than the time between the addition of the next product. It should be noted that the pump pressure and therefore the velocity in the main channel was determined for maximum operator control. First, the time between each channel was calculated. Using the Dolomite Mitas P-pump mentioned earlier, the possible pressure range in the main channel is 0-145 psi with a resolution of 0.01 psi (http://www.dolomite-

microfluidics.com/webshop/pressure-pumps-modules-c-38_41_42/mitospump-p-724). Choosing a very low pressure (to correlate to a very low velocity) of 0.05 psi, the flow rate can be determined using the Hagen-Poiseuille equation (derived from the Navier-Stokes equations), which applies to Newtonian fluids in laminar and incompressible flow, as seen in equation 1. For this system, ΔP_s, which represents the pressure loss due to skin friction throughout the channel, is equal to the pressure introduced by the pump to maintain constant flow (0.05 psi). The main channel is assumed to be cylindrical, and its radius, r, is 50 microns. The viscosity of the fluid, η, is 0.001002 Pa*s since the fluid is water, and the length of the main channel, l, is 0.06 meters.

$$F = \frac{\Delta P_s \pi r^4}{8\eta l} \quad (1)$$

With the aforementioned inputs, the flow rate, F, is equal to 1.4×10^{-11} m^3/s (or 0.84 microliters/minute), which corresponds to a velocity of 0.00179 m/s. For the specific microfluidic chip proposed in figure 20, the time for each GUV to travel past all four channels at this velocity is 33.52 seconds, meaning that there is an 8.38 second delay between the addition of each reactant to the GUV. This flow rate corresponds to a throughput of 7 GUVs/minute, which is an extremely fast production rate. However, this is a conservative throughput for this system since it is based on an extremely slow flow rate. As mentioned previously, it is possible for this system to become automated in the future for the even more rapid production of synthetic cells or other components. If this were the case, the flow rate in the main channel could be drastically increased with regard to the

maximum ability of the automated optical trapping system. However, since the flow in the main channel should remain laminar, it is recommended that the Reynolds number for microfluidic flow should be below 100, and for best results, below 1. With the flow rate described above, and with water as the transport medium, the Reynolds number is 0.178 (see Appendix B for calculations). It is recommended that the flow not be increased enough to drastically change the Reynolds number.

It is also important to consider an example reaction, to show that it is possible for reactions to occur through completion before the GUV reaches the next station and a new reactant is introduced. This is necessary in order to avoid unwanted reactions between new reactants and byproducts of the first reaction. As an example, the reaction used in glow sticks was used because of its visible product of reaction. The concentrations were determined as a function of time, so that the reaction progress can be estimated before experimentation. Essentially, hydrogen peroxide and bis(2,4,6-trichlorophenyl)oxalate (TCPO) are added in the presence of a dye (such as DPA). The hydrogen peroxide will oxidize the TCPO to from both trichlorophenol and an unstable peroxyacid ester. The peroxyacid ester will decompose into phenol and 1,2-dioxetanedione. After time, the 1,2-dioxetandione will degrade to produce carbon dioxide, and as a result of the degradation, the dye will become excited and exhibit fluorescent light (Fogler 2006). As it emits light, it is assumed that the excited dye will revert back to its inactive state. This four-step reaction is written out below, where the * indicates that the dye is excited:

$$hydrogen\ peroxide + TCPO \rightarrow peroxyacid\ ester$$

$$peroxyacid\ ester \rightarrow 2\ phenol + 1{,}2\ dioxetanedione$$

$$1{,}2\ dioxetanedione + dye \rightarrow 2\ carbon\ dioxide + dye* + light$$

$$dye* \rightarrow dye$$

For the sake of calculations, the pseudo-steady-state hypothesis (PSSH) is used. This implies that an active intermediate (the excited dye) is reacting as fast as it is forming, and is reverting back to its unexcited state as soon as light is emitted (Fogler 2006). Additionally, the phase change occurring in the production of carbon dioxide is ignored, and is assumed to have little effect on the resulting concentration equations (Fogler 2006). Finally, it is assumed that the concentration of excited dye is proportional to the light emitted, and that the fluorescence due to the excitement of the dye is observable at the start of carbon dioxide production.

The reaction rate equations were written for the above four-step reaction using the following variables as representatives for each of the products and reactants:

$$A + B \overset{k_1}{\rightarrow} D$$

$$D \overset{k_2}{\rightarrow} 2C + E$$

$$E + F \xrightarrow{k_3} 2H + K + light$$

$$K \xrightarrow{k_4} F$$

The rate constants for each step are represented by k_1, k_2, k_3, and k_4. For the creation of the reaction rate equations, it was assumed that the reaction steps occur in only one direction, and that all are elementary reactions. The reaction rate equations were determined for each component and are written below in equations 2-9.

$$r_A = -k_1[A][B] \quad (2)$$

$$r_B = -k_1[A][B] \quad (3)$$

$$r_C = k_2[D] \quad (4)$$

$$r_D = k_1[A][B] - k_2[D] \quad (5)$$

$$r_E = k_2[D] - k_3[E][F] \quad (6)$$

$$r_F = k_4[K] - k_3[E][F] \quad (7)$$

$$r_H = k_3[E][F] \quad (8)$$

$$r_K = k_3[E][F] - k_5[K] \quad (9)$$

The GUV was modeled as a batch reactor (as opposed to a continuous stirred-tank reactor, plug flow reactor, or packed bed reactor), since there is no input or output after the addition of the reactants. It was assumed that the release of reactants was instantaneous,

since a batch reactor model was used, and that the GUV content was well-mixed so that the reaction rate equations were not dependent on space. To determine the concentrations of these components with respect to time, a mass balance was written first. Then, the input and output streams were set to zero (for a more complete set of calculations, refer to Appendix B). The resulting equations matched equation 10 below, and were determined for each component:

$$t = \int_{C_{i,o}}^{C_i} \frac{dC_i}{r_i} \tag{10}$$

To solve these equations in series, it was assumed that the initial concentrations of components C, D, E, H, and K were zero. The initial concentrations of components A and B were set to 0.7 M and 0.8 M, respectively for the following calculations, although could easily be changed in the MATLAB script shown in Appendix A. The initial concentration of the inactivated dye was set to 0.0005 M, according to experimental data (Fogler 2006). The rate constants were set to the following, as obtained from Fogler: k_1=1.485 $M^{-1}s^{-1}$, k_2=1.485 s^{-1}, k_3=0.00891 $M^{-1}s^{-1}$, k_4=0.00111 s^{-1}.

In order to solve this series of equations, they were rewritten in differential form as shown below in equation 11:

$$\frac{dC_i}{dt} = r_i \tag{11}$$

Then, they were solved numerically using finite steps to estimate the derivative as shown in equation 12.

$$\frac{df}{dx} \approx \frac{f(x+\Delta x)-f(x)}{\Delta x} \tag{12}$$

Equations for each component were entered into MATLAB in this form, and were numerically solved simultaneously with a step size (Δx) of 0.09 (MATLAB code can be seen in Appendix A). A graph was obtained and can be seen in figure 29, below. The graph seems to be a decent representation of the reaction. The concentrations of the reactants A and B are decreasing exponentially as they are used during the first step of the reaction, as shown by the magenta and red lines in the top image. The concentrations of components C and E (green and black lines in the top image) are increased towards the very beginning of the reaction since they are products of the second step, and remain constant since C is not involved in any further steps and E is only reacted with a very small concentration of dye in later steps. The concentration of component D (blue line in the top image) is increased during the first step of the reaction where it is produced, and eventually decreases as it is used as a reactant in the second step. Individual graphs for components F, H, and K can also be seen in figure 29, since they are better visible on much smaller concentration scales. In the middle, left image of figure 29, it can be seen that the concentration of F begins at 0.0005 M and slowly decreases as it becomes activated and later deactivated. In the middle, right image, the concentration of H can be shown increasing as it is produced in the third reaction step. Finally, in the bottom image of figure 29, the concentration of the activated dye can be seen increasing as light is being emitted. The concentration of any desired

component (A, B, C, D, E, F, H, or K) at any time can be determined by using MATLAB to read specific points off of the graph. It is important to note that the reaction seems to reach completion after about four seconds (with the aforementioned initial concentrations and k values). The rate of reaction for light production is also a function of temperature. For every 10 degrees F increase, the rate will double (Fogler 2006). However, it is difficult to obtain concentrations as high as 0.8 M using a liposome delivery system. Ideal concentration curves (like those shown below) may require the delivery of reactants via multiple liposomes.

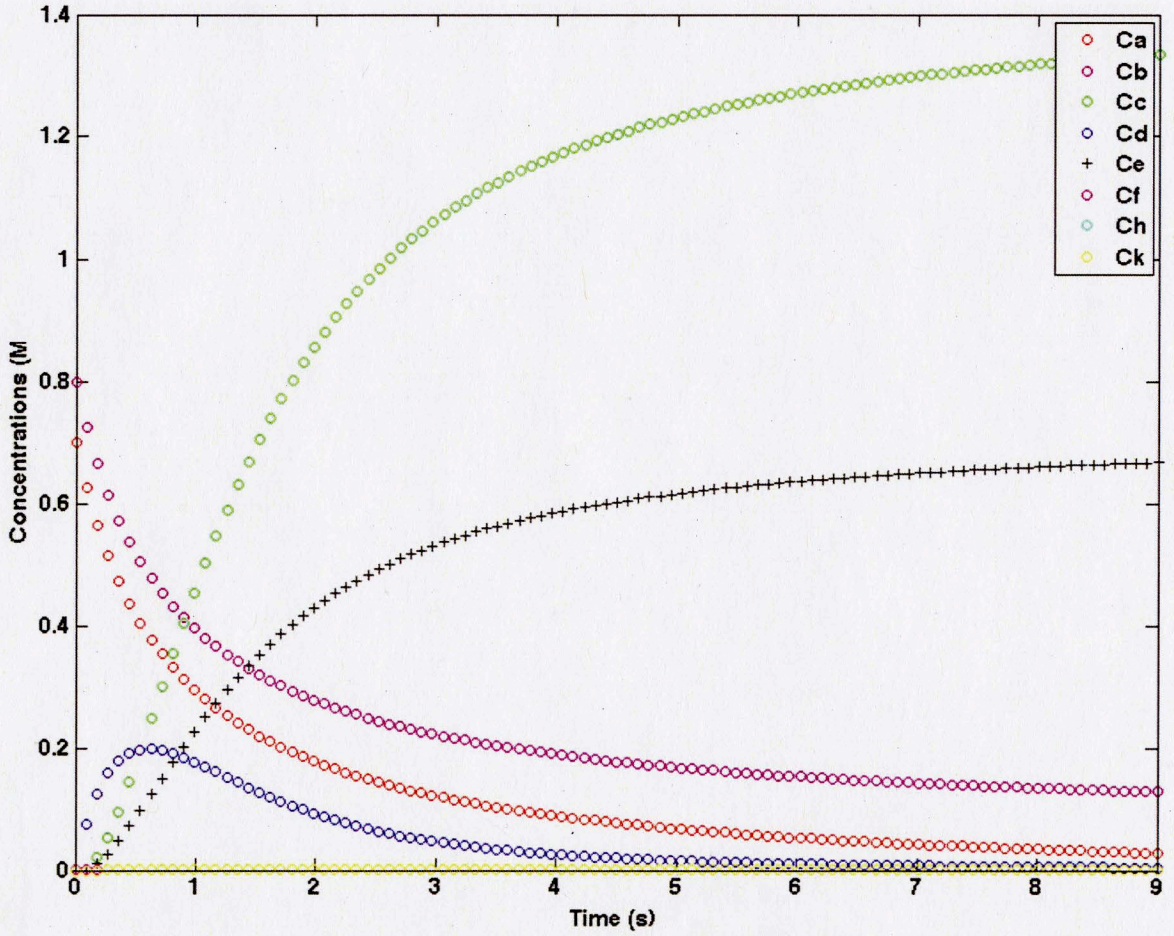

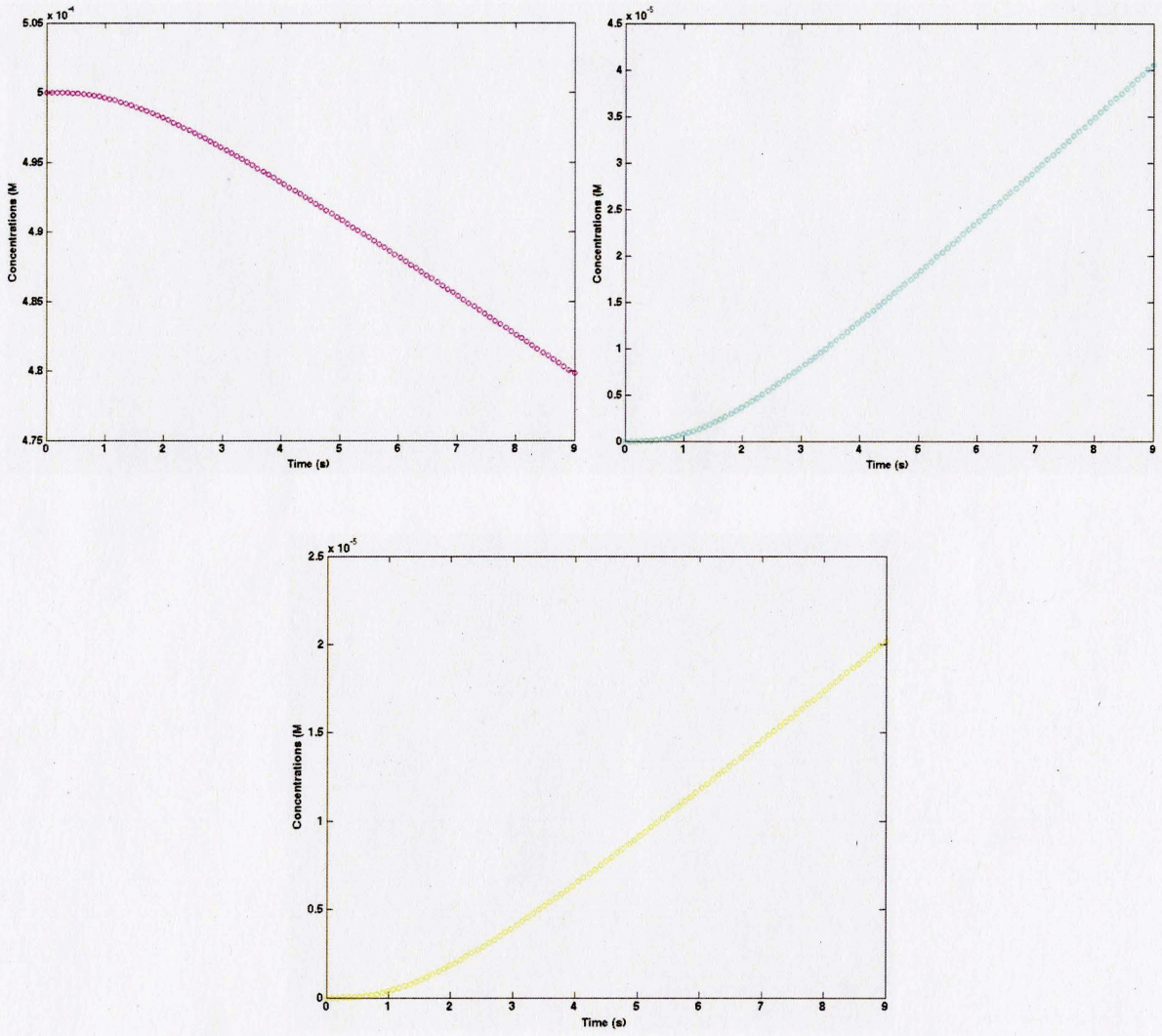

Figure 29. Graph of the concentrations (in M for the top graph, $Mx10^{-4}$ for the middle left graph, and $Mx10^{-5}$ for the middle right and bottom graphs) of the components from the above reaction with respect to time (in s) (Graph created by MATLAB code in Appendix A).

These calculations are beneficial for future work done with this system, as they can help to predict the reaction time and concentrations of components as a function of time in the GUVs. Reaction rate equations can easily be written for any proposed reaction, and can be

plugged into the MATLAB script along with initial concentrations to obtain a graph like the one in figure 29.

Although this reaction was used to create an initial model for the assembly line system, it is not one that could practically be implemented due to the high concentrations that are necessary to achieve the reaction in a reasonable amount of time (about 0.8 M). A concentration this high is difficult to obtain because the reactants are delivered in liposomes that are about 125 million times smaller (by volume) than the GUV to which they are deposited. This results in an extremely large dilution factor, which cannot easily be overcome, as it would be impractical to deliver millions of content-filled liposomes to each GUV. A reaction that is possible, however, is one that can be controlled and vastly sped-up enzymatically. Due to their enormous catalytic power, enzymes can accelerate reaction rates by as much as 10^{16}, even in extremely dilute solutions (Garrett 1999). For the sake of calculations, it was assumed that a 10^{16} increase in reaction rate corresponded to a 10^{16} increase in the rate constant for the first step of the reaction, k_1. Any limitations as a result of diffusion time, which may result in a lower rate constant, were assumed to be negligible (so the Damköhler number was assumed to be less than 1). Enzyme-controlled reactions are often found in natural cells, which again affirms the proposed system's natural affinity for biological processes. The concentration profiles in figure 29 can be altered to better represent biological systems by choosing lower initial molar concentrations and higher rate constants, which are representative of enzyme activity. A new concentration profile

with these changes can be seen in figure 30. Note that the general shape of each concentration curve has remained as expected, although the concentrations are plotted at a much lower scale.

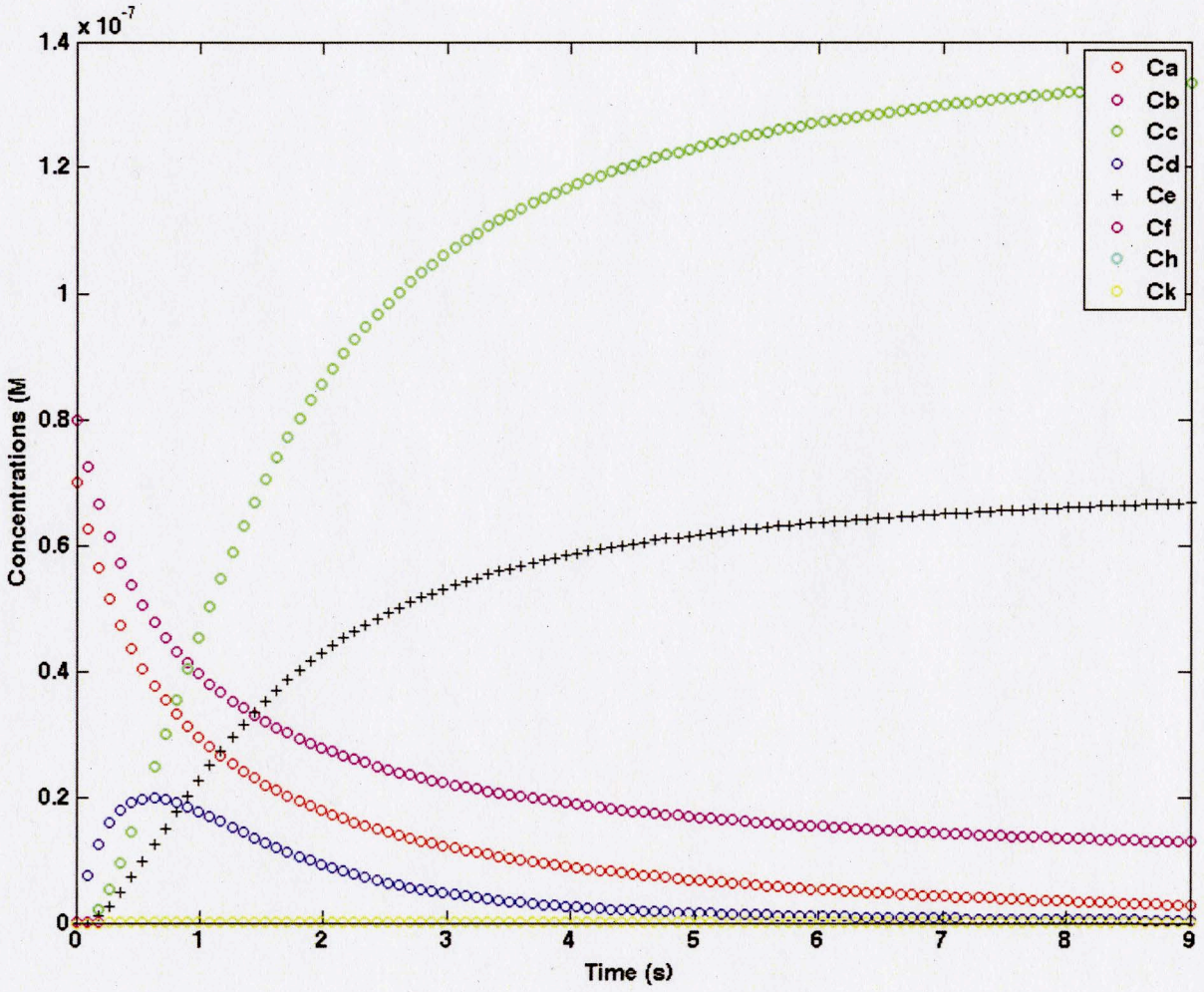

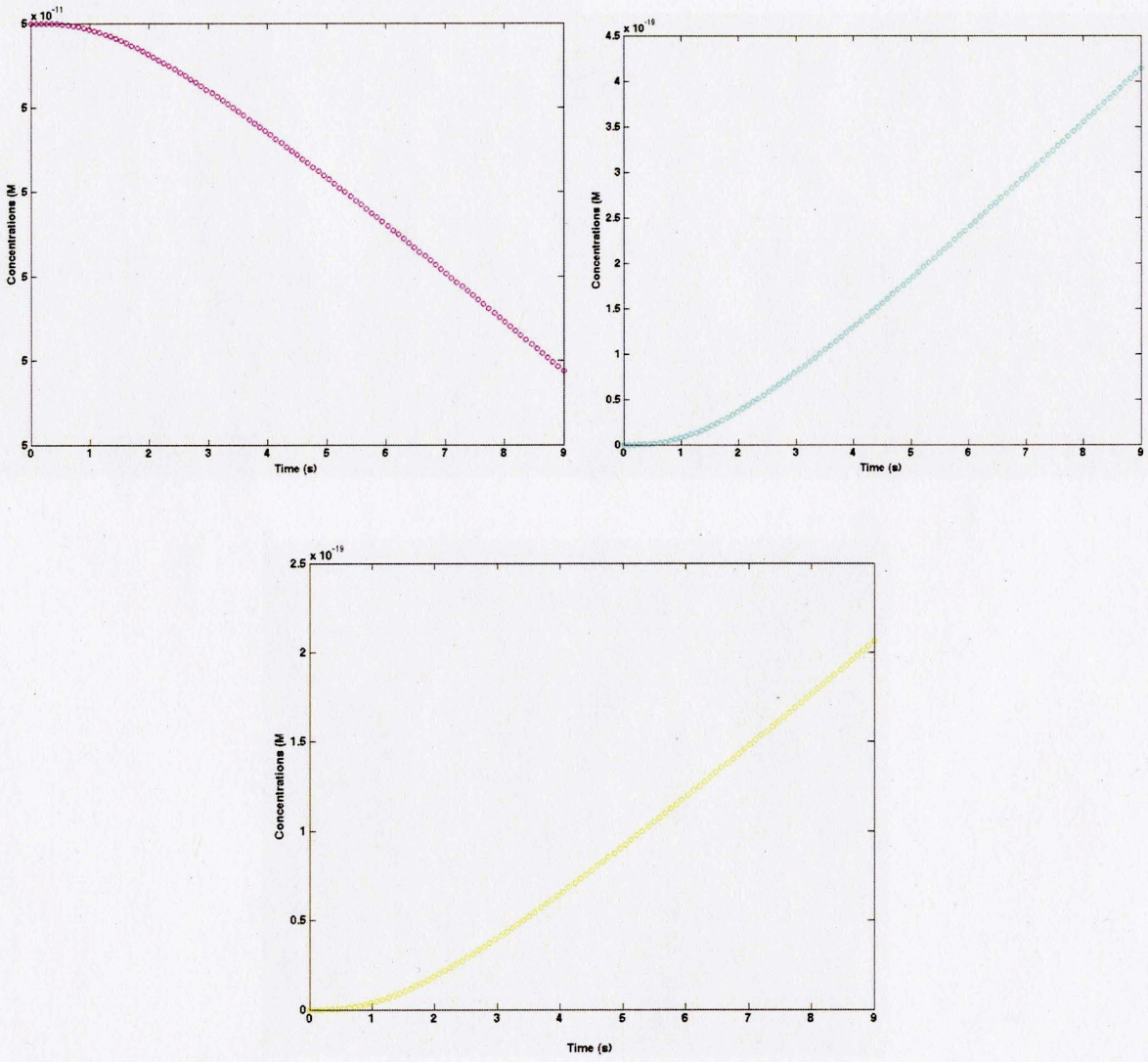

Figure 30. A graph of the concentrations (in $Mx10^{-7}$ for the top graph, $Mx10^{-11}$ for the middle left graph and $Mx10^{-19}$ for the middle right and bottom graphs) of the components in the above reaction vs. time (in s) if the initial molar concentrations are set to $A_0=0.7x10^{-7}$ M, $B_0=0.8x10^{-7}$ M, $F_0=0.0005x10^{-7}$ M, and k_1 is set to $1.485x10^{7}$ $M^{-1}s^{-1}$ to better represent a biological system.

Finally, another beneficial experiment would be the assembly of nucleic acid fragments (the largest fragments that can fit into a gold-coated liposome) into a complete genome by

delivering the fragments along with ligase into a synthetic membrane in the presence of ATP. It is necessary to ensure that the chosen fragments have ends such that they can be combined before this experiment takes place. This should first be confirmed outside of the microfluidic chip before this method is attempted. One possible issue with this experiment is the ability of the segments to join without the presence of naturally occurring cellular enzymes. If this system were used to load genome segments into a natural cell, then it would be much simpler. However, the overall goal is to be able to make a synthetic membrane come to life, so it should be determined which naturally occurring components are required for the joining of nucleic acid segments in an artificial membrane in the presence of ligase and ATP. Aside from being a simple experiment to prove that the assembly line system works, the combination of DNA or RNA segments would also be significant in that it would link this system to the synthetic biology field and more closely associate the design with the idea of a synthetic cell. It would demonstrate the possibility of effectively introducing a man-made genome into a man-made membrane.

Potential Benefits

Although the suggested system is novel, other groups are trying to achieve the same thing: a system that can be used to efficiently load membranes with specific content. Photoporation, optical injection, and optical transfection are examples of currently used methods that this new technique could hypothetically replace. Photoporation is the placement of a sub-micron hole in a cell membrane; optical injection is the introduction of

membrane-impermeable substances into these holes; and optical transfection is the insertion of nucleic acids into these pores (Marchington 2010). The Dholakia group in the U.K. is well known for their optical trapping methods, and have used optical traps to make the aforementioned three processes more efficient (Marchington 2010). Similar to the system described in this report, the group designed a microfluidic system that automates the optical injection of cells, although they use photoporation techniques to do so. The authors claim an impressive injection rate of 1 cell/second with the use of a femtosecond laser, which is a great improvement to previous methods. However, the system still depends on optical injection, meaning that it relies on the uptake of the surrounding fluid by the cells that have undergone photoporation. So, the surrounding fluid must contain the nanoparticles that are meant to be loaded into the cell. This creates a problem with specificity, since this method cannot be used to load specific particles, but rather, whatever particles are contained in the surrounding solution. Each microfluidic chip system could only be used to load one type of nanoparticle at a time if specificity is a requirement.

Other research groups have noted that microfluidic technology and synthetic biology go hand in hand. Since the main problem in synthetic biology is the understanding of complex biological systems, microfluidic technology is an appealing option because biological responses can be observed and tested on a cellular level (Vinuselvi 2011). Furthermore, a microfluidic system allows for these studies to be autonomous and multiplexed (Vinuselvi 2011). In their recent review article "Microfluidic technologies for synthetic biology,"

Vinuselvi and Lee have noted lab groups that have been able to take full advantage of these properties and designed microfluidics systems that integrate optical and electrical components into a microfluidic chip (Vinuselvi 2011). In the future, the microfluidic chip proposed in this report could be modified to include components such as those mentioned in Vinuselvi's review paper.

The production of synthetic cells could be within reach if the system described in this paper were used. Through the utilization of a microfluidic chip and a spatial light modulator, it would be possible to take the synthetic biology and microfluidic technology connection even further by manipulating multiple liposomes at a time either into cells or within cells in ways that cannot be done using any of the current methods. The ease of the iTweezers application would allow for simplicity in the handling of the liposomes as well as accurate placement in three-dimensions. The proposed system meets all of the original design criteria, which are listed again below:

1. The system is able to accurately and precisely load GUVs with the desired content, and is therefore able to obtain reproducible results
2. The system is able to drastically increase the rate of the insertion of components into GUVs (as applied to synthetic cell production and otherwise)
3. The system is able to be easily integrated into the current lab set-up
4. The system is cost effective

The first is accomplished by utilizing a specific optical trapping system, which is accurate and precise even on subcellular levels and can be proved using one of the proposed experiments described previously. The second criterion is met through the use of a microfluidic chip, which allows for the insertion of components into GUVs in an organized, methodical manner. The throughput of the system, as calculated previously, is very high and allows for the production of 7 GUVs per minute without much effort by the operator, which is an extremely fast pace. The third is demonstrated by the need for only a spatial light modulator, a microfluidic chip and its accessories, and free downloadable software in addition to the current lab equipment. The spatial light modulator the iTweezers software can be easily integrated into the system and the microfluidic chip is simply placed on the current inverted microscope stage. Lastly, the system is cost effective, as it requires only $1,027 for the first custom microfluidic chip and its accessories (and $84 for each subsequent chip), and $18,000 for the spatial light modulator, which can also be utilized for other lab set-ups that require a multiplexed laser beam.

6. Conclusion

If the researchers who will someday be able to synthesize genomes coding for the continuous production of biofuels, artificial skin for burn victims, drugs, or vaccines are able to utilize the proposed system, then their ideal results would be reached much sooner. Cells with these genomes could be mass-produced, and then could be set to self-divide a specific amount of times before programmed cell death occurs, or could be made to self-

divide and replicate until their product is unlimited. The possibilities of cell types are similarly unlimited. Through utilization of the Registry of Standard Biological Parts, it could be possible to build a living biological cell capable of doing almost anything from purely synthetic components. And with the use of this system, the building process could be streamlined and rapid. Markers would ensure the identification of synthetic cells, especially if a universal marking system is used. While this report does not propose a novel idea in the creation of artificial cells, it does introduce a game-changing synthesis process that can be used to create any synthetic cell imaginable.

Appendix A: MATLAB Code

```
k1=1.485;
k2=1.485;
k3=.00891;
k4=.00111;

f1=0.7;
f2=0.8;
f3=0;
f4=0;
f5=0;
f6=0.0005;
f7=0;
f8=0;

tval=(0);
funcvala=(f1);
funcvalb=(f2);
funcvalc=(f3);
funcvald=(f4);
funcvale=(f5);
funcvalf=(f6);
funcvalh=(f7);
funcvalk=(f8);

step=0.09;

for n=step:step:9

a=f1-(step*k1*f1*f2);
b=f2-(step*k1*f1*f2);
c=f3+(2*step*k2*f4);
d=f4+step*(k1*f1*f2-k2*f4);
e=f5+step*(k2*f4-k3*f5*f6);
f=f6+step*(k4*f8-k3*f5*f6);
h=f7+(2*step*k3*f5*f6);
k=f8+step*(k3*f5*f6-k4*f8);

f1=a;
f2=b;
f3=c;
f4=d;
f5=e;
f6=f;
f7=h;
f8=k;

tval=[tval n];
```

```
funcvala=[funcvala f1];
funcvalb=[funcvalb f2];
funcvalc=[funcvalc f3];
funcvald=[funcvald f4];
funcvale=[funcvale f5];
funcvalf=[funcvalf f6];
funcvalh=[funcvalh f7];
funcvalk=[funcvalk f8];

end

%plot(tval, funcvalk, 'yo')
plot(tval, funcvala, 'ro', tval, funcvalb, 'mo', tval, funcvalc, 'go', tval,
funcvald, 'bo', tval, funcvale, 'k+', tval, funcvalf, 'mo', tval, funcvalh,
'co', tval, funcvalk, 'yo')
%axis ([0 9 0 0.0025])
xlabel('Time')
ylabel('Concentrations')
legend('Ca', 'Cb', 'Cc', 'Cd', 'Ce', 'Cf', 'Ch', 'Ck')
```

Appendix B: Calculations

Reynolds number:

$$Re = \frac{Lv\rho}{\mu}$$

Where L is equal to the diameter of the channel if it is assumed to be cylindrical, v is equal to the average velocity, as determined using equation 1, ρ is equal to the density of the medium in the channels (1000 kg/m^3 for water), and μ is equal to the viscosity of the medium (0.001002 Pa*s for water).

Mass balance:

$$in - out + generation = accumulation$$

$$F_{i0} - F_i + \int r_i dV = \frac{dN_i}{dt}$$

The two equations above are true for all reactor systems. Here, N_i is defined as the number of moles of component I, V is the volume, F is the flow rate, and r_i is the reaction rate of component i. For a batch reactor, the flow rates F_{io} and F_i are equal to zero since there are no inlet or outlet streams. Due to the aforementioned assumption that the reaction rate is not dependent on space, and that the inlet and outlet flows are zero, the equation for a batch reactor can be seen below:

$$r_i V = \frac{dN_i}{dt}$$

Furthermore, since concentration is defined as moles/volume, it can be written as:

$$r_i V = V\frac{dC_i}{dt}$$

which can be simplified to:

$$r_i = \frac{dC_i}{dt}$$

for each component $C_A(t)$, $C_B(t)$, $C_C(t)$, $C_D(t)$, $C_E(t)$, $C_F(t)$, $C_H(t)$, and $C_K(t)$. These equations can then be solved for residence time by integrating:

$$t = \int_{C_{io}}^{C_i} \frac{dC_i}{r_i}$$

Plugging in equations 2-9 obtains the following equations:

$$t = -\int_{C_{A0}}^{C_A} \frac{dC_A}{k_1 C_A C_B}$$

$$t = -\int_{C_{B0}}^{C_B} \frac{dC_B}{k_1 C_A C_B}$$

$$t = \int_{C_{C0}}^{C_C} \frac{dC_C}{2k_2 C_D}$$

$$t = \int_{C_{D0}}^{C_D} \frac{dC_D}{k_1 C_A C_B - k_2 C_D}$$

$$t = \int_{C_{E0}}^{C_E} \frac{dC_E}{k_2 C_D - k_3 C_E C_F}$$

$$t = \int_{C_{F0}}^{C_F} \frac{dC_F}{k_4 C_K - k_3 C_E C_F}$$

$$t = \int_{C_{H0}}^{C_H} \frac{dC_H}{2k_3 C_E C_F}$$

$$t = \int_{C_{K0}}^{C_K} \frac{dC_K}{k_3 C_E C_F - k_4 C_K}$$

Since each concentration is a function of time, these equations must be solved numerically.

Finite Step Integration:

The best way to solve these equations was determined to be via finite step integration using MATLAB. This method uses the following equation to estimate a solution:

$$\frac{df}{dx} \approx \frac{f(x+\Delta x)-f(x)}{\Delta x}$$

In order to fit this equation, the 5 equations above were written in differential form:

$$\frac{dC_A}{dt} = -k_1 C_A C_B$$

$$\frac{dC_B}{dt} = -k_1 C_A C_B$$

$$\frac{dC_C}{dt} = 2k_2 C_D$$

$$\frac{dC_D}{dt} = k_1 C_A C_B - k_2 C_D$$

$$\frac{dC_E}{dt} = k_2 C_D - k_3 C_E C_F$$

$$\frac{dC_F}{dt} = k_4 C_K - k_3 C_E C_F$$

$$\frac{dC_H}{dt} = 2k_3 C_E C_F$$

$$\frac{dC_K}{dt} = k_3 C_E C_F - k_4 C_K$$

These equations were then combined with the finite step integration equation to establish the following 5 equations, which were then input into MATLAB and were solved.

$$f_1[2] = f_1[1] - \Delta x k_1 f_1[1] f_2[1]$$

$$f_2[2] = f_2[1] - \Delta x k_1 f_1[1] f_2[1]$$

$$f_3[2] = f_3[1] + 2\Delta x k_2 f_4[1]$$

$$f_4[2] = f_4[1] + \Delta x(k_1 f_1[1] f_2[1] - k_2 f_4[1])$$

$$f_5[2] = f_5[1] + \Delta x(k_2 f_4[1] - k_3 f_5[1] f_6[1])$$

$$f_6[2] = f_6[1] + \Delta x(k_4 f_8[1] - k_3 f_5[1] f_6[1])$$

$$f_7[2] = f_7[1] + 2\Delta x k_3 f_5[1] f_6[1]$$

$$f_8[2] = f_8[1] + \Delta x(k_3 f_5[1] f_6[1] - k_4 f_8[1])$$

Here, $f_i[1]$ represents the concentration of component i at some time t; $f_i[2]$ represents the concentration of component i at time=t+Δx and is represented by simply the component letter in the program. (Numbers 1, 2, 3, 4, 5, 6, 7, and 8 correspond to components A, B, C, D, E, F, H, and K respectively). The boundary conditions for the problem were set so that the initial concentrations of components C, D, E, H, and K were zero, so that the following equation is true:

$$C_A(0) + C_B(0) + C_F(0) = C_A(t) + C_B(t) + C_C(t) + C_D(t) + C_E(t) + C_F(t) + C_H(t) + C_K(t)$$

Finally, these equations and the boundary conditions along with the rate constants were entered into MATLAB to create the script displayed in Appendix A. The code can be changed to represent any reaction, as long as the initial concentrations, rate constants, and reaction rate equations are altered to correctly represent the reaction.

Works Cited

Atkinson, M.R., Savageau, M.A., Myers, J.T., Ninfa, A.J. "Development of genetic circuitry exhibiting toggle switch or oscillatory behavior in Escherichia coli." *Cell*, 2003; 113: 597-607.

Barani, H., Montazer, M. "A review on applications of liposomes in textile processing." *Journal of Liposome Research*, 2008; 18(3): 249-262.

Benner, Steven A. , Sismour, A. Michael. "Synthetic biology." *Nature*, 2005; 6: 533-543.

Bolinger, P.Y., Stamou, D., Vogel, H. "An integrated self-assembled nanofluidic system for controlled biological chemistries." *Angew. Chem. Int. Ed.*, 2008; 47: 5544-5549.

Bowman, R., Gibson, G., Padgett, M. "Particle tracking stereomicroscopy in optical tweezers: Control of trap shape." *Optics Express*, 2010; (18) 11: 11785-11790.

Bowman, R.W., Gibson, G., Carberry, D., Picco, L., Miles, M., Padgett, M.J. "iTweezers: optical micromanipulation controlled by an Apple iPad." *J. Opt.*, 2011; 044002.

Bowman, R., Preece, D., Gibson, G., Padgett, M. "Stereoscopic particle tracking for 3D touch, vision, and closed-loop control in optical tweezers." *J. Opt.*, 2011; 044003.

Church, G.M., Gilbert, W. "Genomic sequencing." *Proc. Natl. Acad. Sci. USA*, 1984; 81: 1991-1995.

Deamer, D. "Life After the Synthetic Cell." *Nature*, 2010; 465(27): 422-424.

Ellis, T., Wang, C., Collins, J.J. "Diversity-based, model-guided construction of synthetic gene networks with predicted functions." *Nature Biotechnol*, 2009; 27: 465-471.

Estes, D.J., Mayer, M. "Giant liposomes in physiological buffer using electroformation in a flow chamber." *Biochimica et Biophysica Acta*, 2005; 1712: 152-160.

Fogler, H.S. "Elements of Chemical Reaction Engineering: 4th Edition." *Prentice-Hall Inc.*, 2006.

Fortina, P., Kricka, L.J., Surrey, S., Grodzinski, P. "Nanobiotechnology: the promise and reality of new approaches to molecular recognition." *Trends in Biotechnology*, 2005; 23(4): 168-173.

Friedland, A., Lu, T., Wang, X., Shi, D., Church, G., Collins, J.J. "Synthetic Gene Networks that Count." *Science*, 2009; 324: 1199-1202.

Gardner, T.S., Cantor, C.R., Collins, J.J. "Construction of a genetic toggle switch in Escherichia coli." *Nature*, 2000; 403: 339-342.

Garrett, R., Grisham, C. "Biochemistry." Brooks Cole; 2nd edition. October, 1999.

Gibson, D.G., Glass, J.I., Lartigue, C., Noskov, V.N., Chuang, R.Y., Algire, M.A., Benders, G.A., Montague,M.G., Ma, L., Moodie, M.M., Merryman, C., Vashee, S., Krishnakumar, R., Assad-Garcia, N., Andrews-Pfannkoch, C., Denisova, E.A., Young, L., Qi, Z.Q., Segall-Shapiro, T.H., Calvey, C.H., Parmar, P.P., Hutchison, C.A., Smith, H.O., Venter, J.C. "Creation of a Bacterial Cell Controlled by a Chemically Synthesized Genome." *Science*, 2010; 329: 52-56.

Goeddel, D.V., Kleid, D.G., Bolivar, F., Heyneker, H.L., Yansura, D.G., Crea, R., Hirose, T., Kraszewski, A., Itakura, K., Riggs, A.D. "Expression in Escherichia coli of chemically synthesized genes for human insulin." *Proceedings of the National Academy of Sciences of the United States of America*, 1979; 76(1): 106-110.

Gonnet, G.H, Cohen, M.A, Benner S.A. "Exhaustive matching of the entire protein-sequence database." *Science*, 1992; 256: 1443-1445.

http://www.apple.com/ipad/

http://www.biotec.tu-dresden.de/cms/index.php?id=199

http://biotech.rpi.edu/index.php/facilities/microscopy/283

http://cheme.berkeley.edu/faculty/keasling/

http://www.dolomite-microfluidics.com/webshop/pressure-pumps-modules-c-38_41_42/mitospump-p-724

http://en.wikipedia.org/wiki/File:Liposome.jpg

http://en.wikipedia.org/wiki/Polarizer

http://en.wikipedia.org/wiki/Poly(methyl_methacrylate)

http://ffame.org/sbenner.php

http://www.holoeye.com/download_daten/Spatial_Light_Modulator_LC-R_720.pdf

http://www.holoeye.com/spatial_light_modulators-technology.html

http://www.hms.harvard.edu/dms/BBS/fac/church.php

http://igem.org/

http://itunes.apple.com/us/app/itweezers/id456952257?mt=8

http://www.jcvi.org/cms/about/overview/

http://www.news-medical.net/health/Liposome-Uses.aspx

http://partsregistry.org/Main_Page

http://www.pharmainfo.net/reviews/overview-brain-targeting-drug-delivery-system

http://www.physics.gla.ac.uk/Optics/projects/tweezers/software/

http://www.plluisi.org/

http://ptonline.aip.org/journals/doc/PHTOAD-ft/vol_62/iss_2/26_1.shtml?bypassSSO=1

http://www.sciencedaily.com/releases/2010/03/100311101612.htm

http://www.synbiosafe.eu/index.php?page=synthcells

http://www.topas.com/topas_brochure_english.pdf

http://www.turnkey-solutions.com.au/cam_prosilica_gc640_camera.htm

http://www.viewsfromscience.com/documents/webpages/nanocrystals.html

Jiang, E., He, X., Chen, X., Sun, G., Wu, H., Wei, Y., Zhao, X. "Expression of CD40 in ovarian cancer and adenovirus-mediated CD40 ligand therapy on ovarian cancer in vitro." *Tumori*, 2008: 94(3): 356-361.

Karlsson, M., Davidson, M., Karlsson, R., Karlsson, A., Bergenholtz, J., Konkoli, Z., Jesorka, A., Lobovkina, T., Hurtig., J., Voinova, M., Orwar, O. "Biomimetic nanoscale reactors and networks." *Annual Review of Physical Chemistry*, 2004; 55: 613-649.

Korlach, J., Schwille, P., Webb WW., Feigenson, G.W. "Characterization of lipid bilayer phases by confocal microscopy and fluorescence correlation spectroscopy." *Proceedings of the National Academy of Sciences of the United States of America*, 1999; 96:8461-8466.

Kwok, R. "Five hard truths for synthetic biology." *Nature,* 2010; 463.

Leung, S.J. BME Forum Presentation. 2011.

Leung, S.J, Kachur, X.M., Bobnick, M.C., Romanowski, M. "Wavelength-selective light-induced release from plasmon resonant liposomes." *Advanced Functional Materials*, 2011; 21: 1113-1121.

"Life After the Synthetic Cell." *Nature*, 2010; 465(27):422-424.

Luisi, P.L. "Does Science See A Purpose In Life?" *Center for Theoretical Study,* 1998.

Luisi, P.L. "Enzymes hosted in reverse micelles in hydrocarbon solution." *Angewandte Chemie*, 1985; 24(6): 439-528.

Luisi, P.L. "The Emergence of Life: From Chemical Origins to Synthetic Biology." Cambridge University Press. 2006.

Luisi, P.L., Chiarabelli, C. "Chemical Synthetic Biology." Wiley. 2011.

Luisi, P.L., Stano, P. "The Minimal Cell: The Biophysics of Cell Compartment and the Origin of Cell Functionality." Springer. 2011.

Luisi, P.L., Stano, P. "Vesicle Behavior: In Search of Explanations." *Journal of Physical Chemistry B*, 2008; 112: 14655-14664.

Marchington, R.F., Arita, Y., Tsampoula, X., Gunn-Moore, F.J., Dholakia, K. 'Optical injection of mammalian cells using a microfluidic platform." *Biomedics Optics Express,* 2010; 1(2): 527-537.

Merkle, D., Kahya, N., Schwille, P. "Reconstitution and anchoring of cytoskeleton inside giant unilamellar vesicles." *ChemBioChem*, 2008; 9:2673-2681.

Meure, L.A., Knott, R., Foster, N.R., Dehghani, F. "The depressurization of an expanded solution into aqueous media for the bulk production of liposomes." *Langmuir*, 2009; 25: 326-337.

Microfluidic ChipShop. "Lab-on-a-Chip Catalogue." 09/2011.

Mouritsen, O.G. "Lipids, curvature, and nano-medicine." *Eur. J. Lipid Sci. Technol.,* 2011; 113: 1174-1187.

Neuman, K.C., Block, S.M. "Optical Trapping." *Review of Scientific Instruments,* 2004; 75(9): 2787-2809.

O'Brien, D.F., Costa, L.F., Ott, R.A. "Photochemical functionality of rhodopsin-phospholipid recombinant membranes." *Biochemistry,* 1977; 16(7): 1295-1303.

Padgett, M., and Bowman, R. "Tweezers with a Twist." *Nature Photonics*, 2011; 5:343-348.

Piccirilli, J.A., Krauch, T., Moroney, S.E., Benner, S.A. "Enzymatic incorporation of a

new base pair into DNA and RNA extends the genetic alphabet." *Nature*, 1990; 343: 33-37.

Pramanik, J., Keasling, J.D. "Stoichiometric model of Escherichia coli metabolism: Incorporation of growth-rate dependent biomass composition and mechanistic energy requirements." *Biotechnology and Bioengineering*, 1997; 56(4): 398-421.

Purnick, P., and Weiss, R. "The second wave of synthetic biology: from modules to systems." *Nature*, 2009; 10:410-422.

Quotation, Conoptics Inc, 2011

Quotation, Holoeye, 2011

Quotation, Hamamatsu, 2011

Quotation, Leeds Precision Instruments, 2011

Quotation, Laser Quantum, 2010

Rasmussen, S. "Life After the Synthetic Cell." *Nature*, 2010; 465(27):422-424.

Ro, D.K., et al. "Production of the antimalarial drug precursor artemisinic acid in engineered yeast." *Nature*, 2006; 440: 940-943.

Savage, N. "Digital spatial light modulators." *Nature Photonics*, 2009; 3: 170-172.

Schwille, P. "Bottom-up synthetic biology: engineering in a tinkerer's world." *Science*, 2011; 333:1252-1254.

Schwille, P., Diez, S. "Synthetic biology of minimal systems." *Biochemistry and Molecular Biology*, 2009; 44(4):223-242.

Schwille, P., Haupts, U., Maiti, S, et al. "Molecular dynamics in living cells observed by fluorescence correlation spectroscopy with one- and two-photon excitation." *Biophysical Journal*, 1999; 77(4): 2251-2265.

Schwille, P., MeyerAlmes, F.J., Rigler, R. "Dual-color fluorescence cross-correlation spectroscopy for multicomponent diffusional analysis in solution." *Biophysical Journal*, 1997; 72(4): 1878-1886.

Stachowiak, J.C., Richmond, D.L., Li, T.H., Liu, A.P., Parekh, S.H., Fletcher D.A. "Unilamellar vesicle formation and encapsulation by microfluidic jetting." *Proceedings of the National Academy of Science*, 2008; 105 (12): 4697-4702.

Stano, P., Luisi, P.L. "Achievements and open questions in the self-reproduction of vesicles and synthetic minimal cells." *Chemical Communications*, 2010; 46: 3639-3653.

Stojanovic, M.N., Stefanovic, D. "A deoxyribozyme-based molecular automaton." *NatureBiotechnology*, 2003; 21: 1069-1074.

Szostak, J.W., Bartel, D.P., Luisi, P.L. "Synthesizing Life." *Nature*, 2001; 409: 387-390.

Tabor, J.J., Salis, H.M., Simpson, Z.B., Chevalier, A.A., Levskaya, A., Marcotte, E.M., Voigt, C.A., Ellington, A.D. "A synthetic genetic edge detection program." *Cell*, 2009; 137: 1272-1281.

Tsumoto, K., Nomura, S.M., Nakatani, Y., Yoshikawa, K. "Giant Liposome as a Biochemical Reactor: Transcription of DNA and Transportation by Laser Tweezers." *Langmuir*, 2001; 27: 7225-7228.

Troutman, T.S., Barton, J.K., Romanowski, M. "Biodegradable plasmon resonant nanoshells." *Advanced Materials,* 2008; 20:2604-2608.

Turkbey, B., Kobayashi, H., Ogawa, M., Bernardo, M., Choyke, P. "Imaging of Tumor Angiogenesis: Functional or Targeted?" *Nuclear Medicine and Molecular Imaging*, 2009; 193:304-313.

Venter, J.C., Adams, M.D., Myers E.W. "The sequence of the human genome." *Science*, 2001; 291: 1304-+.

Vinuselvi, P., Park, S., Kim, M., Park, J.M., Kim, T., Lee S.K. "Microfluidic technologies for synthetic biology." *International Journal of Molecular Sciences,* 2011; 12: 3576-3593.

White, K.A., Chengelis, D.A., Gogick, K.A., Stehman, J., Rosi N.L., Petoud, S. "Near-infrared luminescent lanthanide MOF barcodes." *Journal of the American Chemical Society,* 2009; 131 (50): 18069-+.

Yuan, F., Dellian, M., Fukumura, D., Leunig, M., Berk, D.A., Torchilin, V.P., Jain, R.K. "Vascular-permeability in a human tumor xenograft- Molecular-size dependence and cutoff size." *Cancer Research,* 1995; 55 (17): 3752-3756.